Empowerment for Continuous Agent-Environment Systems

Department of Computer Science
Technical Report AI-10-03
The University of Texas at Austin

Tobias Jung[1]
tjung@cs.utexas.edu

Daniel Polani[2]
d.polani@herts.ac.uk

Peter Stone[1]
pstone@cs.utexas.edu

[1]Department of Computer Science
University of Texas at Austin
1616 Guadalupe, Suite 2408
Austin, Texas 78701
USA

[2]Adaptive Systems and Algorithms Research Groups
School of Computer Science
University of Hertfordshire
1 College Lane
Hatfield AL10 9AB, Herfordshire
United Kingdom

Empowerment for Continuous Agent-Environment Systems

Technical Report AI-10-03

Draft September 30, 2010

Abstract

This paper develops generalizations of *empowerment* to continuous states. Empowerment is a recently introduced information-theoretic quantity motivated by hypotheses about the efficiency of the sensorimotor loop in biological organisms, but also from considerations stemming from curiosity-driven learning. Empowemerment measures, for agent-environment systems with stochastic transitions, how much influence an agent has on its environment, but only that influence that can be sensed by the agent sensors. It is an information-theoretic generalization of joint controllability (influence on environment) and observability (measurement by sensors) of the environment by the agent, both controllability and observability being usually defined in control theory as the dimensionality of the control/observation spaces. Earlier work has shown that empowerment has various interesting and relevant properties, e.g., it allows us to identify salient states using only the dynamics, and it can act as intrinsic reward without requiring an external reward. However, in this previous work empowerment was limited to the case of small-scale and discrete domains and furthermore state transition probabilities were assumed to be known. The goal of this paper is to extend empowerment to the significantly more important and relevant case of continuous vector-valued state spaces and initially unknown state transition probabilities. The continuous state space is addressed by Monte-Carlo approximation; the unknown transitions are addressed by model learning and prediction for which we apply Gaussian processes regression with iterated forecasting. In a number of well-known continuous control tasks we examine the dynamics induced by empowerment and include an application to exploration and online model-learning.

Keywords: Information theory, learning, dynamical systems, self-motivated behavior

Short title: Empowerment for Continuous Agent-Environment Systems

1 Introduction

One goal of AI research is to enable artificial agents (either virtual or physical ones) to act "intelligently" in complex and difficult environments. A common view is that intelligent behavior can be "engineered"; either by fully hand-coding all the necessary rules into the agent, or by relying on various optimization-based techniques to automatically generate it. For example, in modern control and dynamic programming a human designer specifies a performance signal which explicitly or implicitly encodes goals of the agent. By behaving in a way that optimizes this quantity, the agent then does what the programmer wants it to do. For many applications, this is a perfectly reasonable approach that can lead to impressive results. However, it typically requires some prior knowledge and sometimes subtle design by the human developer to achieve sensible or desirable results.

In this paper, we investigate an approach to use the "embodiment" of an agent (i.e., the dynamics of its coupling to the environment) to generate preferred behaviors without having to resort to specialized, hand-designed solutions that vary from task to task. Our research embraces the related ideas of self-organization and self-regulation, where we aim for complex behavior to derive from simple and generic internal rules. The philosophy is that seemingly intentional and goal-driven behavior emerges as the by-product of the agent trying to satisfy universal rules rather than from optimizing externally defined rewards. Examples of this kind of work include *homeokinesis* (Ay, Bertschinger, Der, Güttler, & Olbrich, 2008; Der, Steinmetz, & Pasemann, 1999; Der, 2000, 2001; Zahedi, Ay, & Der, 2010), or the work in (Still, 2009). The second idea is that of intrinsically motivated behavior and artificial curiosity (Schmidhuber, 1991), where an agent engages in behavior because it is inherently "interesting" or "enjoyable", rather than as a step towards solving a specific (externally defined) goal. Intrinsically motivated behavior may not directly help in solving a goal, but there are indications that it leads to exploration and allows an agent to acquire a broad range of abilities which can, once the need arises, be easily molded into goal-directed behavior. Related relevant publications include, for example, (Singh, Barto, & Chentanez, 2005). Other related work can be found in (Lungarella, Pegors, Bulwinkle, & Sporns, 2005; Lungarella & Sporns, 2005; Sporns & Lungarella, 2006; Lungarella & Sporns, 2006) and (Prokopenko, Gerasimov, & Tanev, 2006; Steels, 2004; Kaplan & Oudeyer, 2004).

Here we will consider the principle of *empowerment* (Klyubin, Polani, & Nehaniv, 2005a, 2008), an information-theoretic quantity which is defined as the channel capacity between an agent's actions and its sensory observations in subsequent time steps. Empowerment can be regarded as "universal utility" which defines an a priori intrinsic reward or rather, a value/utility for the states in which an agent finds itself in. Empowerment is fully specified by the dynamics of the agent-environment coupling (namely the transition probabilities); a reward does not need to be specified. It was hypothesized in (Klyubin et al., 2005a, 2008) that the greedy maximization of empowerment would direct an agent to "interesting" states in a variety of scenarios:

- For one, empowerment can be considered a stochastic generalization of the concept of *mobility* (i.e., number of options available to an agent) which is a powerful heuristic in many deterministic and discrete puzzles and games. Being in a state with high empowerment gives an agent a wide choice of actions — conversely, if an agent in "default mode" poises itself a priori in a high-empowerment state, it is best equipped to quickly move from there into a variety of target states in an emergency (for example, in the game of soccer, a goalkeeper who is about to receive a penalty kick and has no prior knowledge about the player behavior to expect naturally positions himself in the middle of the goal). In this regard the quantity of empowerment allows an agent to automatically (without explicit external human input) identify those states, even in complex environments.

- In the present paper we show that, for a certain class of continuous control problems, empowerment provides a natural utility function which imbues its states with an a priori value, without an

explicit specification of a reward. Such problems are typically those where one tries to keep a system "alive" indefinitely, i.e., in a certain goal region for as long a time as possible. On the other hand, choosing the wrong actions or doing nothing would instead lead to the "death" of the system (naturally represented by zero empowerment). A natural example is pole-balancing. [1] In this context, we will find the smoothness of the system informs the local empowerment gradients around the agent's state of where the most "alive" states are. Choosing actions such that the *local* empowerment score is maximized would then lead the agent into those states. In the pole-balancing example this means that for a wide range of initial conditions, the agent would be made to balance the pendulum.

Previous studies with empowerment showed promise in various domains but were essentially limited to the case of small-scale and finite-state domains (the ubiquitous gridworld) and furthermore, state transition probabilities were assumed to be known a priori. The main contribution of this article is to extend previous work to the significantly more important case of (1) continuous vector-valued state spaces and (2) initially unknown state transition probabilities. The first property means that we will be able to calculate empowerment values only approximately; more specifically, here we will use Monte-Carlo approximation to evaluate the integral underlying the empowerment computation. The second property considers the case where the state space is previously unexplored and implies that the agent has to use some form of online model-learning to estimate transition probabilities from *state-action-successor state* triplets it encounters while interacting with the environment. Here, we will approach model-learning using Gaussian process regression with iterated forecasting.

To summarize, the paper is structured into three parts as follows:

1. The first part, Section 2, gives a first, informal definition of empowerment and illustrates its general properties in a well-known finite-state domain.

2. The second part forms the main technical portion. Section 3 starts with a formal definition of empowerment for the continuous case and gives an algorithm for its computation based on Monte-Carlo approximation of the underlying high-dimensional integrals. Section 4 describes model-learning using Gaussian process regression (GPs) – however, since this itself is a rather complex subject matter, for brevity here we cannot go beyond a high-level description.

3. The third part examines empowerment empirically in a number of continuous control tasks well known in the area of reinforcement learning. The experiments will demonstrate how empowerment can form a natural utility measure, and how states with high empowerment values coincide with the natural (and intuitive) choice of a goal state in the respective domain. This way, if we incorporate empowerment into the perception-action loop of an agent, e.g., by greedily choosing actions that lead to the highest empowered states, we can obtain a seemingly goal-driven behavior. As an application of this, we study the problem of exploration and model-learning: using empowerment to guide which parts of the state-space to exlore next, the agent can quickly "discover the goal" and thus more efficiently explore the environment – without exhaustively sampling the state space.

2 Illustrative example

Although a more formal definition of empowerment will follow in the next section, here we will start by motivating it through a toy example. Informally, empowerment computes for any state of the environment

---

[1]Empowerment in the pole-balancing example was first investigated in (Klyubin et al., 2008) with a discretized state space and *a priori* known state transition probabilities. Here we will strongly extend this example to the continuous case and online learning. State transition probabilities are initially not known. Instead, the agent has to learn the transition probabilities while interacting with the environment.

the logarithm of the *effective* number of successor states the agent can induce by its actions. Thus empowerment essentially measures to what extent an agent can influence the environment by its actions: it is zero if, regardless what the agent does, the outcome will be the same. And it is maximal if every action will have a *distinct*[2] outcome. Note that empowerment is specifically designed to allow for more general stochastic environments, of which deterministic transitions are just a special case.
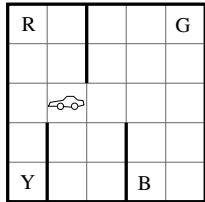
As an example, consider the taxi-domain (Dietterich, 1998), a well-known problem in reinforcement learning with finite state and action space and stochastic transitions. The environment, shown on the left, consists of a 5×5 gridworld with four special locations designated 'R','Y','G','B'. Apart from the agent ("the taxi"), there is a passenger who wants to get from one of the four locations to another (selected at random). The state of the system is the x, y coordinate of the agent, the location of the passenger (one of 'R','Y','G','B','in-the-car') and its destination (one of 'R','Y','G','B'). Overall there are $500 = 5 \times 5 \times 5 \times 4$ distinct states. Usually in RL, where the interest is on abstraction and hierarchical learning, a factored representation of the state is used that explicitly exploits the structure of the domain. For our purpose, where identifying salient states is part of the problem, we do not assume that the structure of the domain is known and will use a flat representation instead. The agent has six possible elementary actions: the first four ('N','S',E','W') move the agent in the indicated direction (stochastically, there is a 20% chance for random movement). If the resulting direction is blocked by a wall, no movement occurs. The agent can also issue a pick-up and drop-off action, which require that the taxi is at the correct location and (in the latter case) the passenger is in the car. Issuing pick-up and drop-off when the conditions are not met does not result in any changes. If a passenger is successfully delivered, the environment is reset: the agent is placed in the center and a passenger with new start and destination is generated.

Using these state transition dynamics, we compute the 3-step empowerment, i.e., the *effective* number of successor states reachable over an action horizon of 3 steps (meaning we consider compound actions of a sequence of three elementary actions) for every state of the system. Figure 1 shows some of the results: the values are ordered such that every subplot shows the empowerment values that correspond to a specific slice of the state space. For example, the top left subplot shows the empowerment value of all x, y locations if the passenger is waiting at 'Y' and its destination is 'G', which with our labeling of the states corresponds to states 376-400. Inspecting the plots, two things become apparent: for one, in general, locations in the center have high empowerment (because the agent has freedom to move wherever it wants); locations in the corners have low empowerment (because the agent has only limited choices of what it can do). More interesting is the empowerment value at the designated locations: if a passenger is waiting at a certain location, its empowerment, and that of its neighbors 2 steps away, increases. Similarly, if a passenger is in the car, the empowerment of the destination, and that of its neighbors 2 steps away, increases. The reason is that in both situations the agent now has additional, previously unavailable, ways of affecting the environment (plot (c) and (d) have a higher relative gain in empowerment, because they result in the end of an episode, which teleports the agent to the center). Thus these states stand out as being "interesting" under the heuristic of empowerment. Incidentally, these are also exactly the subgoal states if the agent's task were to transport the passenger from source to destination. Note that here we did not have to specify external reward or goals, as empowerment is intrinsically computed from the transition dynamics alone.

Empowerment essentially "discovers" states where additional degrees of freedom are available, and creates a basin of attraction around them, indicating salient features of the environment of interest to the agent. It is not difficult to imagine an agent that uses empowerment as a guiding principle for exploration; e.g., by choosing in each state greedily the action that leads to the successor state with the highest empowerment. We expect that such an agent would traverse the state space in a far more sensible

---

[2]Meaning that for discrete state spaces, the sets of successor states are disjoint for differerent actions; for continuous state spaces, the domains of the underlying pdfs are non-overlapping.

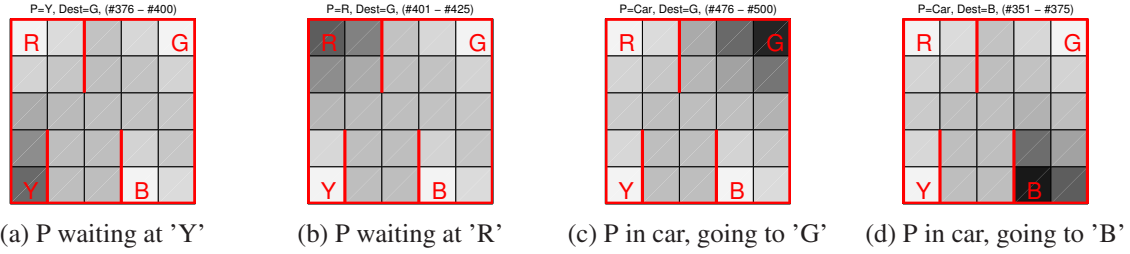| (a) P waiting at 'Y' | (b) P waiting at 'R' | (c) P in car, going to 'G' | (d) P in car, going to 'B' |

Figure 1: Plotting *empowerment* for a subset of states (here locations) for the taxi domain. For clarity, every plot shows the mean-subtracted empowerment (3-step) of a certain slice of the state space, where white corresponds to low empowerment (1.55 nats), and black corresponds to high empowerment (2.75 nats).

way than blind random exploration, as following the trail of increasing empowerment would quickly lead to the discovery of the salient states in the environment. In the remainder of the paper, we will develop methods for carrying over this idea into the continuum and demonstrate how empowerment supersedes typical hand-designed rewards in a number of established benchmark domains.

3 Computation of empowerment

This section defines empowerment formally and gives an algorithm for its computation.

3.1 General definition of empowerment

Empowerment (Klyubin et al., 2005a) is defined for stochastic dynamic systems where transitions arise as the result of making a decision, e.g. such as an agent interacting with an environment. Here we will assume a vector-valued state space $\mathcal{X} \subset \mathbb{R}^D$ and (for simplicity) a discrete action space $\mathcal{A} = \{1, \ldots, N_A\}$. The transition function is given in terms of a density[3] $p(\mathbf{x}_{t+1}|\mathbf{x}_t, a_t)$ which denotes the probability of going from state $\mathbf{x}_t$ to $\mathbf{x}_{t+1}$ when making decision a_t. While we assume the system is fully defined in terms of these 1-step interactions, we will also be interested in more general n-step interactions. Thus, for $n \geq 1$, we consider the sequence $\vec{a}_t^n = (a_t, \ldots, a_{t+n-1})$ of n single-step actions and the induced probability density $p(\mathbf{x}_{t+n}|\mathbf{x}_t, \vec{a}_t^n)$ of making the corresponding n-step transition.

For notational convenience we can assume that, without loss of generality, 1-step and n-step actions are equivalent: let the set of possible n-step actions be formed through exhaustive enumeration of all possible combinations of 1-step actions. If N_A is the number of possible 1-step actions in every state, the number of n-step actions is then $N_n := (N_A)^n$. With this approach, we can consider the system as evolving at the time-scale of n-step actions, so that n-step actions can be regarded as 1-step actions at a higher level of decision making. This abstraction allows us to treat 1-step and n-step actions on equal footing, which we will use to simplify the notation and drop references to the time index. Instead of writing $p(\mathbf{x}_{t+n}|\mathbf{x}_t, \vec{a}_t^n)$ we will now just write $p(\mathbf{x}'|\mathbf{x}, \vec{a})$ to denote the transition from $\mathbf{x}$ to $\mathbf{x}'$ under $\vec{a}$, irrespective of whether $\vec{a}$ is an n-step action or 1-step action. Furthermore we will use the symbol ν to loop over actions $\vec{a}$.

Let $\mathcal{X}'$ denote the random variable associated with $\mathbf{x}'$ given $\mathbf{x}$. Assume that the choice of a particular action $\vec{a}$ is also random and modeled by random variable $\mathcal{A}$. The *empowerment* $C(\mathbf{x})$ of a state $\mathbf{x}$

---

[3]Note that we have to consider stochastic transitions in the continuum. Otherwise if, for every action, the resulting successor states are distinct, empowerment always attains the maximum value. In practice this will usually be the case when simulating continuous control tasks with deterministic dynamics. In this case we artificially add some zero mean Gaussian noise with small variance (see Section 5.2). This can be interpreted as modeling limited action or sensoric resolution, depending on the take. It is also a natural assumption for a robot realized in hardware.
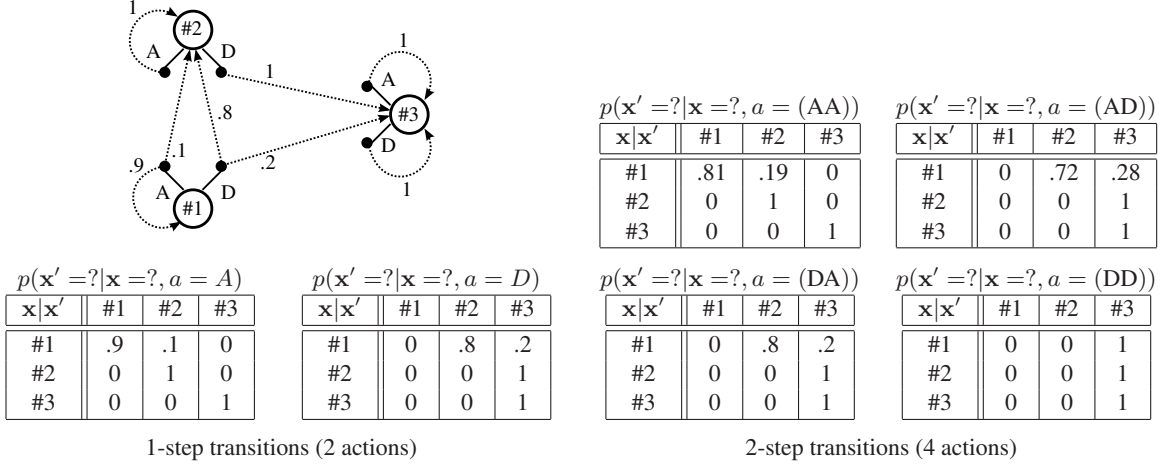
Figure 2: Transition probabilities for a concrete numerical example (see text)

Tables within the figure:

$p(\mathbf{x}' =? | \mathbf{x} =?, a = (AA))$

$\mathbf{x}|\mathbf{x}'$	#1	#2	#3
#1	.81	.19	0
#2	0	1	0
#3	0	0	1

$p(\mathbf{x}' =? | \mathbf{x} =?, a = (AD))$

$\mathbf{x}|\mathbf{x}'$	#1	#2	#3
#1	0	.72	.28
#2	0	0	1
#3	0	0	1

$p(\mathbf{x}' =? | \mathbf{x} =?, a = A)$

$\mathbf{x}|\mathbf{x}'$	#1	#2	#3
#1	.9	.1	0
#2	0	1	0
#3	0	0	1

$p(\mathbf{x}' =? | \mathbf{x} =?, a = D)$

$\mathbf{x}|\mathbf{x}'$	#1	#2	#3
#1	0	.8	.2
#2	0	0	1
#3	0	0	1

$p(\mathbf{x}' =? | \mathbf{x} =?, a = (DA))$

$\mathbf{x}|\mathbf{x}'$	#1	#2	#3
#1	0	.8	.2
#2	0	0	1
#3	0	0	1

$p(\mathbf{x}' =? | \mathbf{x} =?, a = (DD))$

$\mathbf{x}|\mathbf{x}'$	#1	#2	#3
#1	0	0	1
#2	0	0	1
#3	0	0	1

1-step transitions (2 actions)   2-step transitions (4 actions)

(more precisely, the n-step empowerment) is then defined as the Shannon channel capacity (using the differential entropy) between $\mathcal{A}$, the choice of an action sequence, and $\mathcal{X}'$, the resulting successor state:

$$C(\mathbf{x}) := \max_{p(\vec{a})} I(\mathcal{X}'; \mathcal{A} \,|\, \mathbf{x})$$
$$= \max_{p(\vec{a})} \left\{ H(\mathcal{X}' \,|\, \mathbf{x}) - H(\mathcal{X}' \,|\, \mathcal{A}, \mathbf{x}) \right\}. \tag{1}$$

The maximization of the mutual information is with respect to all possible distributions over $\mathcal{A}$, which in our case means vectors of length N_n of probabilities. The entropy and conditional entropy are given by

$$H(\mathcal{X}'|\mathbf{x}) := - \int_{\mathcal{X}} p(\mathbf{x}'|\mathbf{x}) \log p(\mathbf{x}'|\mathbf{x}) d\mathbf{x}' \tag{2}$$

$$H(\mathcal{X}'|\mathcal{A}, \mathbf{x}) := \sum_{\nu=1}^{N_n} p(\vec{a}_\nu) H(\mathcal{X}'|\mathcal{A} = \vec{a}_\nu, \mathbf{x})$$
$$= - \sum_{\nu=1}^{N_n} p(\vec{a}_\nu) \int_{\mathcal{X}} p(\mathbf{x}'|\mathbf{x}, \vec{a}_\nu) \cdot \log p(\mathbf{x}'|\mathbf{x}, \vec{a}_\nu) d\mathbf{x}'. \tag{3}$$

Strictly speaking, the entropies in Eqs. (2) and (3) are differential entropies (which could be negative) and the probabilities are to be read as probability densities. However, as we always end up using the mutual information, i.e. the difference between the entropies, we end up with well-defined non-negative information values which are always finite due to the limited resolution/noise assumed above. Using $p(\mathbf{x}'|\mathbf{x}) = \sum_{i=1}^{N_n} p(\mathbf{x}'|\mathbf{x}, \vec{a}_i) p(\vec{a}_i)$ in Eqs. (2) and (3), Eq. (1) can thus be written as

$$C(\mathbf{x}) := \max_{p(\vec{a})} \sum_{\nu=1}^{N_n} p(\vec{a}_\nu) \int_{\mathcal{X}} p(\mathbf{x}'|\mathbf{x}, \vec{a}_\nu) \cdot \log \left\{ \frac{p(\mathbf{x}'|\mathbf{x}, \vec{a}_\nu)}{\sum_{i=1}^{N_n} p(\mathbf{x}'|\mathbf{x}, \vec{a}_i) p(\vec{a}_i)} \right\} d\mathbf{x}' \tag{4}$$

Hence, given the density $p(\mathbf{x}'|\mathbf{x}, \vec{a}_\nu)$ for making n-step transitions, *empowerment* is a function $C : \mathcal{X} \to \mathbb{R}^{\geq 0}$ that maps an arbitrary state $\mathbf{x}$ to its empowerment $C(\mathbf{x})$.

3.2 A concrete numerical example

Before we proceed, let us make the previous definition more concrete by looking at a numerical example. To simplify the exposition, the example will be discrete (thus integration over the domain is replaced

by summation). We consider an agent in an environment with three states, labeled #1,#2,#3, and two possible actions, denoted A or D. The dynamics of the environment is fully described by the 1-step transitions shown in Figure 2(left). The right side of the figure shows the corresponding 2-step transitions which are derived from the 1-step transitions; for example, the entry $p(\mathbf{x}' = \#1|\mathbf{x} = \#1, a = (AA))$ is obtained by

$$
\begin{aligned}
p(\mathbf{x}' = \#1|\mathbf{x} = \#1, a = (AA)) &= \sum_{i=\#1}^{\#3} p(\mathbf{x}' = \#1|\mathbf{x} = i, a = A) \cdot p(\mathbf{x}' = i|\mathbf{x} = 1, a = A) \\
&= (.9 \times .9) + (.1 \times 0) + (0 \times 0) = .81.
\end{aligned}
$$

Let us now assume we want to calculate the 2-step empowerment value $C(\#1)$ for state $\mathbf{x} = \#1$. First, consider the 2-step mutual information, $I(\mathcal{X}'; \mathcal{A}|\mathbf{x} = \#1)$, for state $\mathbf{x} = \#1$. According to Eq. (1), we have

$$
\begin{aligned}
I(\mathcal{X}'; \mathcal{A}|\mathbf{x} = \#1) &= p(AA) \cdot \sum_{i=\#1}^{\#3} p(\mathbf{x}' = i|\mathbf{x} = \#1, a = AA) \log\left\{ \frac{p(\mathbf{x}' = i|\mathbf{x} = \#1, a = AA)}{p(\mathbf{x}' = i|\mathbf{x} = \#1)} \right\} \\
&+ p(AD) \cdot \sum_{i=\#1}^{\#3} p(\mathbf{x}' = i|\mathbf{x} = \#1, a = AD) \log\left\{ \frac{p(\mathbf{x}' = i|\mathbf{x} = \#1, a = AD)}{p(\mathbf{x}' = i|\mathbf{x} = \#1)} \right\} \\
&+ p(DA) \cdot \sum_{i=\#1}^{\#3} p(\mathbf{x}' = i|\mathbf{x} = \#1, a = DA) \log\left\{ \frac{p(\mathbf{x}' = i|\mathbf{x} = \#1, a = DA)}{p(\mathbf{x}' = i|\mathbf{x} = \#1)} \right\} \\
&+ p(DD) \cdot \sum_{i=\#1}^{\#3} p(\mathbf{x}' = i|\mathbf{x} = \#1, a = DD) \log\left\{ \frac{p(\mathbf{x}' = i|\mathbf{x} = \#1, a = DD)}{p(\mathbf{x}' = i|\mathbf{x} = \#1)} \right\}.
\end{aligned}
$$

The denominator in the logarithm is calculated for any i via:

$$
\begin{aligned}
p(\mathbf{x}' = i|\mathbf{x} = \#1) &= p(\mathbf{x}' = i|\mathbf{x} = \#1, a = AA) \cdot p(AA) \\
&+ p(\mathbf{x}' = i|\mathbf{x} = \#1, a = AD) \cdot p(AD) \\
&+ p(\mathbf{x}' = i|\mathbf{x} = \#1, a = DA) \cdot p(DA) \\
&+ p(\mathbf{x}' = i|\mathbf{x} = \#1, a = DD) \cdot p(DD)
\end{aligned}
$$

As we can see, the resulting value for $I(\mathcal{X}'; \mathcal{A}|\mathbf{x} = \#1)$ will only depend on the individual probabilities of the actions, $p(AA), p(AD), p(DA), p(DD)$, but not on the transition probabilities as these are fixed for a given environment. One natural choice for the action probabilities could be the uniform distribution. However, for empowerment we try to find an assignment of action probabilities such that the resulting $I(\mathcal{X}'; \mathcal{A})$ value is maximimimized among all possible assignments (an algorithm for this will be given in the next section). Below we have calculated the empowerment values MI (taking uniform distribution over actions) and Em (taking the maximizing distribution over actions) in our example for various time horizons, i.e., 1-step, 2-step, etc. Note that, while empowerment values are logarithmic, for the purpose of illustration the results are given in terms of $\exp(I(\mathcal{X}'; \mathcal{A}))$:

|	1-step		2-step		3-step		4-step		5-step	
State	MI	Em	MI	Em	MI	Em	MI	Em	MI	Em
$\mathbf{x} = \#1$	1.70	1.71	1.93	2.17	1.81	2.10	1.58	2.05	1.38	2.02
$\mathbf{x} = \#2$	2	2	1.75	2	1.45	2	1.26	2	1.14	2
$\mathbf{x} = \#3$	1	1	1	1	1	1	1	1	1	1

The first column, 1-step, illustrates the full range of possible empowerment values. Empowerment in state #3 is zero (here, $1 = \exp(0)$), because all actions in #3 have the same outcome. Empowerment in state #2 is maximal (here 2, corresponding to the two possible 1-step actions), because each action in #2 has a different outcome. In state #1 the set of successor states overlap, thus the empowerment value is in between the two extremes.

As the time horizon increases, we can make the following observations. One is that the empowerment value of #3 always stays at zero, because no matter what the agent does, the outcome will be the same (thus absorbing states are "dead" states). Two, the MI value of #2 goes down, whereas its Em value stays constant (this in fact is an important observation). The reason is that, as the time horizon increases, so does the number of possible (n-step) actions, e.g., $32 = 2^5$ for 5 steps. However, a large number of these actions will bring the agent into #3 from which it cannot escape. Therefore, if all actions contribute in equal parts to the result (which they do in MI, where we assume a uniform distribution), those that lead to zero empowerment will dominate and thus also the end result will be close to zero. On the other hand, the maximization in Em will suppress the effect of indistinguishable actions (assigning zero probability to actions having the same outcome and high probabilities to actions having distinct outcomes) and thus ensure that the two distinct choices in #2 are always correctly identified.

3.3 Empowerment or mutual information?

Let us summarize. Empowerment measures to what extent an agent can influence the environment by its actions. It specifically works for stochastic systems (where state transitions are given in terms of probabilities), but can also apply to deterministic systems (which are just a special case of stochastic systems). Empowerment is zero if, regardless what the agent does, the outcome will be the same (i.e., the outcome distribution for a given successor state $\mathbf{x}'$ is independent of the action). And it is maximal if every action will have a distinct outcome (i.e., the probability that a single outcome is produced by two different actions is zero).

Let us now briefly discuss why the related information-theoretic quantity mutual information, which would largely have the same properties and would be easier to compute, is not as powerful as channel capacity at identifying interesting states of the environment.
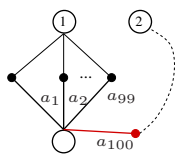
First, let us comment that to use the idea of modeling the influence of the action channel, one has to define some kind of distribution on the actions. As we are considering only an agent's embodiment, but have not defined a controller, there is no default action distribution that one could use. Therefore, one has to distinguish particular action distributions for which the action channel is to be measured. The main natural choices are the choice of an action distribution that is equally distributed, not singling out any particular action, and that one which maximizes $I(\mathcal{X}'; \mathcal{A})$, i.e. the one that achieves channel capacity. As we have seen in the last section, the equidistribution of actions can fail to resolve important properties of the action channel which the optimal distribution does detect. The most obvious situation is one where one has a large number of equivalent actions. If mutual information assumes a uniform distribution over actions, it will be mislead by large numbers of actions that lead to the same outcome. As another example, consider the following situation. Assume an agent has 100 different actions available and is in a state where every action has the same effect (empowerment and mutual information both zero). Now let us assume the agent enters a new state, as shown on the left side, where actions a_1 to a_{99} still have the same outcome (state 1), but one action a_{100} leads to a different state (state 2). In this case, use of mutual information with equidistributed would still be close to zero (≈ 0.05 nats), indicating that all actions roughly have the same effect, whereas empowerment correctly identifies two distinct choices ($\approx 0.69 = \log(2)$ nats) since it will redistribute the actions in a way that highlights the additional degrees of freedom attained by a_{100}.

3.4 Computing empowerment when a model is available

Next we describe the Blahut-Arimoto algorithm for computing the channel capacity given in Eq. (4). For now we assume that the (n-step) transition probabilities $p(\mathbf{x}'|\mathbf{x}, \vec{a}_\nu)$ are known for all actions $\vec{a}_\nu, \nu = 1, \ldots, N_n$.

3.4.1 Blahut-Arimoto algorithm

The Blahut-Arimoto algorithm (Blahut, 1972) is an EM-like algorithm that iterates over distributions $p_k(\vec{a})$, where k denotes the k-th iteration step, to produce the distribution $p^*(\vec{a})$ that achieves the maximum in Eq. (4). Since we consider a discrete action domain, $p_k(\vec{a})$ is represented by a vector $p_k(\vec{a}) \equiv \left(p_k^1, \ldots, p_k^{N_n}\right)$. To avoid cluttered notation, we define

$$d_{\nu,k} := \int_{\mathcal{X}} p(\mathbf{x}'|\mathbf{x}, \vec{a}_\nu) \log \left[\frac{p(\mathbf{x}'|\mathbf{x}, \vec{a}_\nu)}{\sum_{i=1}^{N_n} p(\mathbf{x}'|\mathbf{x}, \vec{a}_i) p_k^i} \right] d\mathbf{x}'. \tag{5}$$

We start with an initial distribution $p_0(\vec{a})$ which is chosen using the uniform distribution, that is $p_0^\nu := 1/N_n$ for $\nu = 1, \ldots, N_n$. At each iteration $k \geq 1$, the probability distribution $p_k(\vec{a})$ is then obtained from $p_{k-1}(\vec{a})$ as

$$p_k^\nu := z_k^{-1} p_{k-1}^\nu \exp(d_{\nu,k-1}) \quad \nu = 1, \ldots, N_n \tag{6}$$

where z_k is a normalization ensuring that the new probabilities sum to one, i.e.

$$z_k = \sum_{\nu=1}^{N_n} p_{k-1}^\nu \exp(d_{\nu,k-1}). \tag{7}$$

Once $p_k(\vec{a}) \equiv \left(p_k^1, \ldots, p_k^{N_n}\right)$ is computed for iteration k, we can use it to obtain an estimate $C_k(\mathbf{x})$ for the empowerment $C(\mathbf{x})$ given in Eq. (4) via

$$C_k(\mathbf{x}) = \sum_{\nu=1}^{N_n} p_k^\nu \cdot d_{\nu,k}. \tag{8}$$

The algorithm in Eqs. (6)-(8) can either be carried out for a fixed number of iterations, or it can be stopped once the change $|C_k(\mathbf{x}) - C_{k-1}(\mathbf{x})| < \varepsilon$ drops below a chosen threshold and hence $C_k(\mathbf{x})$ is reasonably close to $C(\mathbf{x})$.

One problem still remains, which is the evaluation of the high-dimensional integral over the state space in $d_{\nu,k}$.

3.4.2 Monte-Carlo integration

Taking a closer look at Eq. (5), we note that $d_{\nu,k}$ can also be written as expectation with regard to the density $p(\mathbf{x}'|\mathbf{x}, \vec{a}_\nu)$. Assuming that each density $p(\mathbf{x}'|\mathbf{x}, \vec{a}_\nu)$ is of a simple form (e.g. parametric, like a Gaussian or a mixture of Gaussians) from which we can easily draw N_{MC} samples $\{\tilde{\mathbf{x}}'_{\nu,i}\}$, we have

$$\forall \nu : \quad d_{\nu,k} \approx \frac{1}{N_{MC}} \sum_{j=1}^{NMC} \log \left[\frac{p(\tilde{\mathbf{x}}'_{\nu,j}|\mathbf{x}, \vec{a}_\nu)}{\sum_{i=1}^{N_n} p(\tilde{\mathbf{x}}'_{\nu,j}|\mathbf{x}, \vec{a}_i) p_k^i} \right] \tag{9}$$

3.4.3 Example: Gaussian model

As an example consider the case where $p(\mathbf{x}'|\mathbf{x}, \vec{a}_\nu)$ is a multivariate Gaussian (or at least reasonably well approximated by it) with known mean vector $\boldsymbol{\mu}_\nu = \left(\mu_{\nu,1}, \ldots, \mu_{\nu,D}\right)^\mathsf{T}$ and covariance matrix $\boldsymbol{\Sigma}_\nu = \mathrm{diag}\left(\sigma_{\nu,1}^2, \ldots, \sigma_{\nu,D}^2\right)$, which in short will be written as

$$\mathbf{x}'|\mathbf{x}, \vec{a}_\nu \sim \mathcal{N}(\boldsymbol{\mu}_\nu, \boldsymbol{\Sigma}_\nu). \tag{10}$$

Note that here both the mean and covariance will depend on the action $\vec{a}_\nu$ and the state $\mathbf{x}$. Samples $\tilde{\mathbf{x}}'_\nu$ from Eq. (10) are easily generated via standard algorithms.

In summary, to compute the empowerment $C(\mathbf{x})$ given state $\mathbf{x} \in \mathcal{X}$ and transition model $p(\mathbf{x}'|\mathbf{x}, \vec{a}_\nu)$, we proceed as follows.

1. **Input:**

   (a) State $\mathbf{x}$ whose empowerment we wish to calculate.

   (b) For every action $\nu = 1, \ldots, N_n$ a state transition model $p(\mathbf{x}'|\mathbf{x}, \vec{a}_\nu)$, each fully defined by its mean $\boldsymbol{\mu}_\nu$ and covariance $\boldsymbol{\Sigma}_\nu$.

2. **Initialize:**

   (a) $p_0(\vec{a}_\nu) := 1/N_n$ for $\nu = 1, \ldots, N_n$.

   (b) Draw N_MC samples $\tilde{\mathbf{x}}'_{\nu,i}$ each, from $p(\mathbf{x}'|\mathbf{x}, \vec{a}_\nu) = \mathcal{N}(\boldsymbol{\mu}_\nu, \boldsymbol{\Sigma}_\nu)$ for $\nu = 1, \ldots, N_n$.

   (c) Evaluate $p(\tilde{\mathbf{x}}'_{\nu,i}|\mathbf{x}, \vec{a}_\mu)$ for all $\nu = 1, \ldots, N_n; \mu = 1, \ldots, N_n; i = 1, \ldots, N_\mathrm{MC}$.

3. **Iterate** $k = 1, 2, \ldots$ (until $|c_k - c_{k-1}| < \mathtt{tol}$ or maximum number of iterations reached)

   (a) $z_k := 0, c_{k-1} := 0$

   (b) For $\nu = 1, \ldots, N_n$

       i. $d_{\nu,k-1} :=$

   $$\frac{1}{N_\mathrm{MC}} \sum_{j=1}^{N_\mathrm{MC}} \log \left[\frac{p(\tilde{\mathbf{x}}'_{\nu,j}|\mathbf{x}, \vec{a}_\nu)}{\sum_{i=1}^{N_n} p(\tilde{\mathbf{x}}'_{\nu,j}|\mathbf{x}, \vec{a}_i) p_{k-1}(\vec{a}_i)} \right]$$

       ii. $c_{k-1} := c_{k-1} + p_{k-1}(\vec{a}_\nu) \cdot d_{\nu,k-1}$
       iii. $p_k(\vec{a}_\nu) := p_{k-1}(\vec{a}_\nu) \cdot \exp\{d_{\nu,k-1}\}$
       iv. $z_k := z_k + p_k(\vec{a}_\nu)$

   (c) For $\nu = 1, \ldots, N_n$

       i. $p_k(\vec{a}_\nu) := p_k(\vec{a}_\nu) \cdot z_k^{-1}$

4. **Output:**

   (a) Empowerment $C(\mathbf{x}) \approx c_{k-1}$ (estimated).

   (b) Distribution $p(\vec{a}) \approx p_{k-1}(\vec{a})$ achieving the maximum mutual information.

At the end we obtain the estimated empowerment $C_{k-1}(\mathbf{x})$ from c_{k-1} with associated distribution $p_{k-1}(\vec{a}) \equiv \left(p_{k-1}(\vec{a}_1), \ldots, p_{k-1}(\vec{a}_{N_n})\right)$. The computational cost of this algorithm is $\mathcal{O}(N_n^2 \cdot N_\mathrm{MC})$ operations per iteration; the memory requirement is $\mathcal{O}(N_n^2 \cdot N_\mathrm{MC})$. Thus the overall computational complexity scales with the square of the number of (n-step) actions N_n.

4 Model learning

In this section we further reduce our assumptions, and consider an environment for which neither n-step nor 1-step transition probabilities are readily available. Instead, we assume that we could only observe a number of 1-step transitions which are given as triplets of state, performed action, and resulting successor state. Using regression on these samples, we first infer a 1-step transition model. Proceeding from this 1-step model we can then obtain a more general n-step transition model through iteratively predicting n steps ahead in time.

In general, there would be many ways the task of regression could be accomplished. Here we will use Gaussian process regression (GP) (Rasmussen & Williams, 2006). GPs are simple and mathematically elegant, yet very powerful tools that offer some considerable advantages. One is that GPs directly produce a predictive distribution over the target values, which is exactly what is needed in Eq. (4) for the computation of empowerment. Furthermore, the predictive distribution is Gaussian and hence easy to draw samples from during the Monte-Carlo approximation (see Section 3.4.3). Also, GPs are non-parametric, meaning that a GP model is not restricted to a certain class of functions (such as polynomials), but instead encompasses *all* functions sharing the same degree of smoothness. In practice GPs are also very easy to use: the solution can be found analytically and in closed form. The Bayesian framework allows us to nicely address the problem of hyperparameter selection in a principled way, which makes the process of using GPs virtually fully automated, i.e. without having to adjust a single parameter by hand.

4.1 Learning 1-step system dynamics

To learn the state transition probabilities $p(\mathbf{x}'|\mathbf{x}, a = \nu)$, i.e. predict the successor state $\mathbf{x}'$ when performing 1-step action $a = \nu$ in state $\mathbf{x}$, we combine multiple univariate GPs. Each individual $\mathcal{GP}_{\nu j}$, where $j = 1 \ldots D$ and $\nu = 1 \ldots N_A$, predicts the j-th coordinate of successor state $\mathbf{x}'$ under action $a = \nu$. Each individual $\mathcal{GP}_{\nu j}$ is trained independently on the subset of the transitions where action ν was chosen: the desired target outputs we regress on is the change in the state variables (i.e. we predict the difference $\mathbf{x}_{t+1} - \mathbf{x}_t$). Since both state variables and actions are treated separately, we need a total of $D \cdot N_A$ independent GPs.

A detailed description of how univariate regression with GPs work[4] can be found in (Rasmussen & Williams, 2006). Training $\mathcal{GP}_{\nu j}$ gives us a distribution $p(x'_j|\mathbf{x}, a = \nu) = \mathcal{N}(\mu_{\nu j}(\mathbf{x}), \sigma^2_{\nu j}(\mathbf{x}))$ for the j-th variable of the successor state, where the exact equations for the mean $\mu_{\nu j}(\mathbf{x})$ and variance $\sigma^2_{\nu j}(\mathbf{x})$ can be found in (Rasmussen & Williams, 2006). Note that every $\mathcal{GP}_{\nu j}$ will have its own set of hyperparameters $\boldsymbol{\theta}_{\nu j}$, each independently obtained from the associated training data via Bayesian hyperparameter selection. Combining the predictive models for all D variables, we obtain the desired distribution

$$p(\mathbf{x}'|\mathbf{x}, a = \nu) = \mathcal{N}(\boldsymbol{\mu}_\nu(\mathbf{x}), \boldsymbol{\Sigma}_\nu(\mathbf{x})) \tag{11}$$

for making a 1-step transition from $\mathbf{x}$ under action $a = \nu$, where $\boldsymbol{\mu}_\nu(\mathbf{x}) = \big(\mu_{\nu 1}(\mathbf{x}), \ldots, \mu_{\nu D}(\mathbf{x})\big)^\mathsf{T}$, and $\boldsymbol{\Sigma}_\nu(\mathbf{x}) = \mathrm{diag}\big(\sigma^2_{\nu 1}(\mathbf{x}), \ldots, \sigma^2_{\nu D}(\mathbf{x})\big)$. See Figure 3 for an illustration of this situation.

---

[4]There is also the problem of implementing GPs *efficiently* when dealing with a possible large number of data points. For brevity we will only sketch our particular implementation, see (Quiñonero-Candela, Rasmussen, & Williams, 2007) for more detailed information. Our GP implementation is based on the *subset of regressors* approximation. The elements of the subset are chosen by a stepwise greedy procedure aimed at minimizing the error incurred from using a low rank approximation (incomplete Cholesky decomposition). Optimization of the likelihood is done on random subsets of the data of fixed size. To avoid a degenerate predictive variance, the *projected process* approximation was used.

Input: state $\mathbf{x} = (x_1, \ldots, x_D)^\mathsf{T}$, action $a = \nu$

Output: $p(\mathbf{x}'|\mathbf{x}, a = \nu) = \mathcal{N}(\boldsymbol{\mu}_\nu(\mathbf{x}), \boldsymbol{\Sigma}_\nu(\mathbf{x}))$
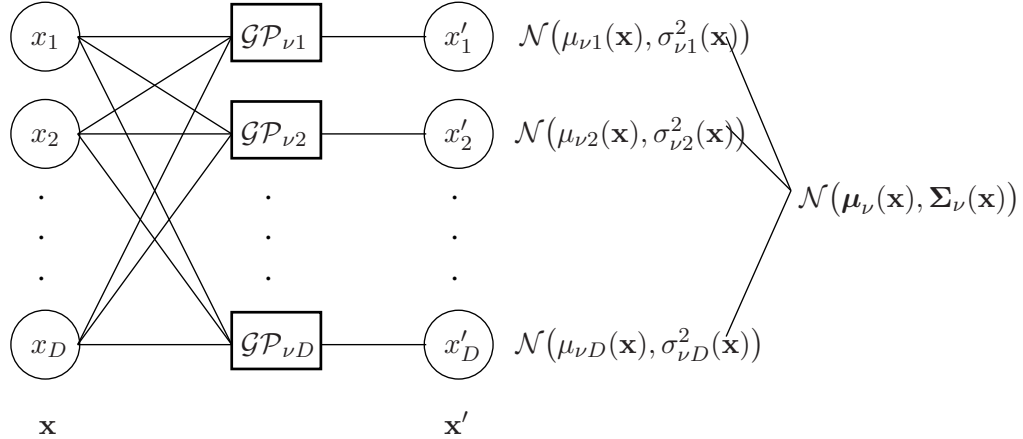
Figure 3: Learning state transition probabilities $p(\mathbf{x}'|\mathbf{x}, a = \nu)$ by combining multiple univariate GPs. Each individual $\mathcal{GP}_{\nu j}$ predicts the j-th coordinate of successor state $\mathbf{x}'$ under action $a = \nu$. Each individual $\mathcal{GP}_{\nu j}$ is trained independently on the corresponding subset of the training data and has its own set of hyperparameters $\boldsymbol{\theta}_{\nu j}$ (obtained from maximizing the marginal likelihood).

4.2 From 1-step to n-step models

To turn the 1-step model into an n-step model $p(\mathbf{x}_{t+n}|\mathbf{x}_t, \vec{a}_t^n)$, where $\vec{a}_t^n = (a_t, a_{t+1}, \ldots, a_{t+n-1})$ is a sequence of n 1-step actions, we have to integrate over all intermediate distributions. Unfortunately, solving this integral analytically in closed form is not possible. One simple approach is again to use sampling methods, like the Monte-Carlo approximation, to numerically determine the integral. Alternatively, one could consider a more sophisticated approximate solution based on the Laplace approximation, as was proposed in (Girard, Rasmussen, Quiñonero-Candela, & Murray-Smith, 2003).

Since, in our experiments, we will only consider very short prediction horizons (typically $n = 3$ or $n = 5$), we will use the more naive approach of predicting iteratively n steps ahead using the learned 1-step model. Given state $\mathbf{x}_t$, we apply Eq. (11) to produce $p(\mathbf{x}_{t+1}|\mathbf{x}_t, a_t)$. Instead of considering the full distribution, we just take its mean $\hat{\mathbf{x}}_{t+1} := \boldsymbol{\mu}_{a_t}(\mathbf{x}_t)$ as point estimate and use that to predict $\mathbf{x}_{t+2}$, applying again the 1-step model Eq. (11) to produce $p(\mathbf{x}_{t+2}|\hat{\mathbf{x}}_{t+1}, a_{t+1})$. Repeating this procedure until the end of the prediction horizon is reached, we obtain after n steps $p(\mathbf{x}_{t+n}|\hat{\mathbf{x}}_{t+n-1}, a_{t+n-1})$ as an approximation to the originally sought n-step transition model $p(\mathbf{x}_{t+n}|\mathbf{x}_t, \vec{a}_t^n)$. In general, this approximation will tend to underestimate the variance of the prediction and produce a slightly different mean, since every time we produce an estimate for $t + i$, we ignore the uncertainty in the preceding prediction for $t + i - 1$. In our case, however, the procedure will incur only a neglible error since the prediction horizon we consider is very short. See (Girard et al., 2003) for more details.

5 Experiments

We have indicated earlier that empowerment has shown intuitively appealing identification of salient states in discrete scenarios and we are now ready to study a number of more intricate continuous scenar-

ios. These scenarios are used as benchmark for typical learning algorithms (e.g., reinforcement learning or optimal control). However, it should be noted that in the latter the learning algorithms need to be instructed about which optimization criterion to use in the learning process. Here, we will always use empowerment maximization as the criterion, and demonstrate that the resulting behaviors actually match closely those where optimization of an external quality criterion is requested. The observation that these behaviors match, is a subtle point and will be discussed in more detail in the discussion (see Section 6).

As an important side effect, empowerment can also be used as a (heuristic) exploration driver in these scenarios: this is particularly interesting since, unlike optimal control algorithms, empowerment is fundamentally local (limited to the horizon defined by the actions) as opposed to optimal control algorithms that, for an informed decision, need to have their horizon extended to encompass information about the desired target state(s) to a sufficiently accurate extent.

Thus, in the following section, we will demonstrate that

1. empowerment *alone* can lead to apparently intentional and goal-directed behavior of an agent based only on the embodiment of the agent with no external reward structure, and

2. how it can furthermore act as a heuristic to guide the agent's exploration of the environment.

We consider two scenarios: one *without model-learning*, and one *with model-learning*. The first scenario will demonstrate that incorporating empowerment into the perception-action loop of an agent produces intuitively desirable behavior, by greedily choosing actions in each state that lead to the highest empowered states. Our primary intent here is to show that empowerment itself is a relevant quantity to be considered and for simplicity we assume that the transition probabilities of the system are known. In the second scenario, we will further reduce our assumptions and consider this no longer to be the case. The agent starts out knowing nothing about the environment it is in. We will then combine empowerment with model-learning and exploration: while, as in the first scenario, the agent chooses its actions based on empowerment, the underlying computations are carried out using a *learned* model for the state transition probabilities. The model is continually updated (in batches) from the transitions the agent experiences and thus gets continually better at predicting the effects the actions will have, which in turn will produce more accurate empowerment values. A comparison with common model-based reinforcement learning, RMAX (Brafman & Tennenholtz, 2002), which operates in a similar fashion but actively optimizes an external performance criterion, concludes.

5.1   The domains

As testbeds for our experiments, we consider simulations of the three physical systems described below. We reiterate that, in the literature, systems like these are usually used in the context of control and learning behavior where a goal (desired target states) is *externally* defined and, by optimizing a thus determined performance criterion, the system is driven to specifically reach that goal. In contrast, empowerment used here is a *generic* heuristic (aimed at curiosity-driven learning) where a goal is not explicitly defined and which operates on innate characteristics of the system's dynamic alone. It will turn out that empowerment intrinsically drives the system (close) to states which in fact are typically externally chosen as goal states. However, with empowerment we do not enforce this goal through any external reward but through a generic intrinsic quantity that, for each domain, is generated in exactly the same way. Note that, in a wider sense, all the tasks belong to the class of control problems where the goal is to choose actions such that the system stays "alive" – to achieve this, the agent has to stay in a certain "stable" goal region. This is a class of problems for which we believe empowerment is particularly well-suited.

Inverted pendulum: The first system consists of a single pole attached at one end to a motor, as depicted in Figure 4. If force is applied, the pole will freely swing in the xy plane. More detailed

dynamic equations of the system are given in the appendix. If no force is applied, the stable equilibrium of the system is when the pole hangs vertically down. Let this state be the initial condition. The goal is to swing up and stabilize the pole in the inverted position. However, the motor does not provide enough torque to do so directly in a single rotation. Instead, the pendulum needs to be swung back and forth to gather energy, before being pushed up and balanced. This creates a somewhat difficult, nonlinear control problem. The state space is 2-dimensional, $\phi \in [-\pi, \pi]$ being the angle, $\dot{\phi} \in [-10, 10]$ the angular velocity. Since our empowerment model only deals with a finite number of 1-step and n-step actions, the control force is discretized to $a \in \{-5, -0.25, 0, 0, +0.25, +0.5\}$.

Riding a bicycle: The second domain we want to apply empowerment to is a more involved one: we consider the bicycle riding task described in (Lagoudakis & Parr, 2003; Ernst, Geurts, & Wehenkel, 2005) and depicted in Figure 4. In this task, a bicycle-rider system (modeled as a simplified mechanical system) moves at a constant speed on a horizontal surface. The bicycle is not self-stabilizing and has to be actively stabilized to be prevented from falling. The goal is to keep the bicycle stable such that it continues to move forward indefinitely. A detailed description of the dynamics of the system is given in the appendix. The problem is 4-dimensional: state variables are the roll angle $\omega \in [-12\pi/180, 12\pi/180]$, roll rate $\dot{\omega} \in [-2\pi, 2\pi]$, angle of the handlebar $\alpha \in [-80\pi/180, 80\pi/180]$, and the angular velocity $\dot{\alpha} \in [-2\pi, 2\pi]$. The control space is inherently 2-dimensional: u_1, the horizontal displacement of the bicycle-rider system from the vertical plane, and u_2, turning the handlebar from the neutral position. Since empowerment can only deal with a finite number of 1-step and n-step actions, we consider 5 possible action vectors: $(u_1, u_2) \in \{(-0.02, 0), (0, 0), (0.02, 0), (0, -2), (0, 2)\}$.

Acrobot: The third domain is the acrobot proposed in (Spong, 1995). The acrobot can be imagined as a gymnast swinging up above a high bar by bending at the hips. As depicted in Figure 4, the acrobot is a two-link robot, which freely swings around the first joint (the hands grasping the bar) and can exert force only at the second joint (the hips). Controlling the acrobot is a very challenging problem in nonlinear control; it is underactuated, meaning that the dimensionality of the state space is higher than that of the actuators, or, informally, that it has more degrees of freedom than actuators (in robotics, many systems are underactuated, including manipulator arms on spacecraft, non-rigid body systems, and balancing systems such as dynamically stable legged robots). Usually two tasks are considered for the acrobot in the literature: the first and easier one is to swing the tip (the feet) of the lower link over the bar at the height of the upper link. The second task is significantly more difficult: as in the first task, the goal is to swing up the lower link; however, this time the acrobot has to reach the inverted handstand position with close to zero velocity, and then to actively balance so as to remain in this highly unstable state for as long as possible. A detailed description of the dynamics of the system is given in the appendix. The initial state of the acrobot is the stable equilibrium with both links hanging vertically down. The state space is 4-dimensional: $\theta_1 \in [-\pi, \pi]$, $\dot{\theta}_1 \in [-4\pi, 4\pi]$, $\theta_2 \in [-\pi, \pi]$, $\dot{\theta}_2 \in [-9\pi, 9\pi]$. Since, as before, empowerment can deal with only a finite number of 1-step and n-step actions, the continuous control was discretized to $a \in \{-1, +1\}$. However, while these two actions alone are sufficient to solve the swing-up task, they are not sufficient for the inverted balance, since for this case, control values between the two extremes -1 and $+1$ must be chosen. Therefore, we include a third, non-primitive 'balance' action, which chooses control values derived from an LQR controller obtained from linearizing the system dynamics about the handstand position (see appendix). Note that this 'balance' action produces meaningful (i.e., actually useful) outputs only very close to the handstand state which means that it cannot be naively used to direct the acrobot to balance from an arbitrary point of the state space.
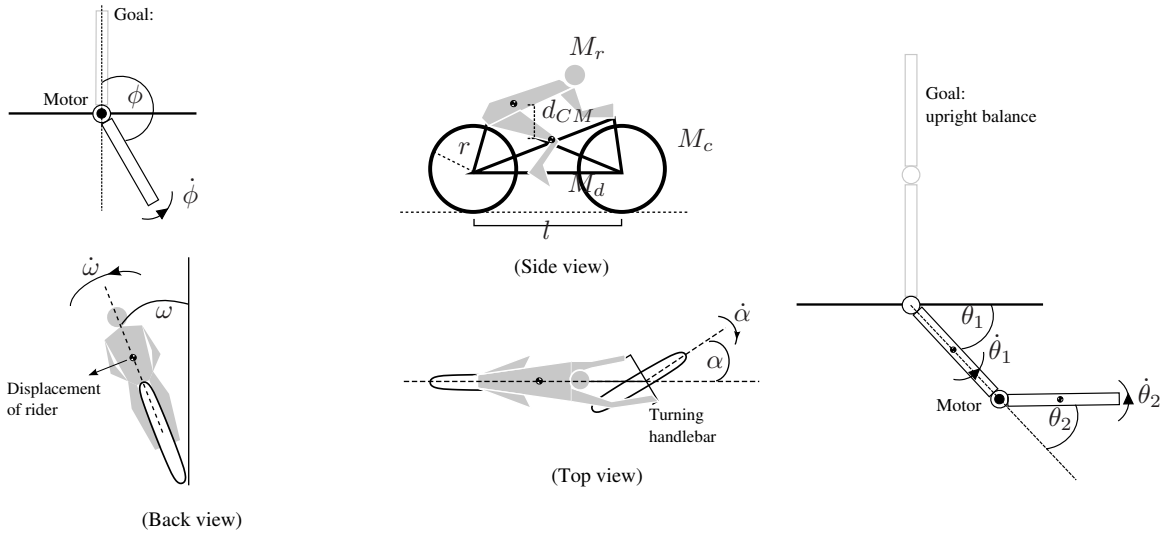
Figure 4: From left to right: the inverted pendulum task, the riding a bicycle task, and the acrobot handstand task.

5.2 First scenario: model-based

In our first series of experiments, the agent chooses actions greedily to maximize empowerment. For all domains, we assume that the state transition probabilities are known. The control loop becomes the following: every time step t the agent observes the current state $\mathbf{x}_t$. Using the state transition function, we determine the 1-step successor states under each of the possible 1-step actions. For each of these states, we compute the empowerment value as described in Section 3.4.3, using $N_{\mathrm{MC}} = 200$, $\mathtt{TOL} = 10^{-5}$ and $\mathtt{MAX\_ITER} = 150$, and adding Gaussian white noise with (state-independent) covariance to "smear out" the otherwise deterministic state transitions. The agent then executes the action corresponding to the successor state with the highest empowerment value (empowerment-greedy action selection), advancing the time and producing the next state $\mathbf{x}_{t+1}$.

Note that in practice, for empowerment values to be meaningful, we usually require an increased look-ahead horizon into the future than just a single simulation step; thus, instead of 1-step empowerment, we usually need to examine n-step empowerment for values of n greater than one. Here we form the n-step actions through exhaustive enumeration; thus if N_A is the number of possible 1-actions the agent has available, the number N_n of n-step actions we have to consider during the computation of empowerment is $N_n = (N_A)^n$. For each experiment performed, we informally determined the minimum time horizon of lookahead necessary to achieve the desired effect. Especially for small simulation steps (such as $\Delta = 0.01$), the number n of 1-step actions needed to fill a given time horizon could grow relatively large, which in turn would then lead to a large number of n-step actions, rendering computational costs prohibitive. To reduce the number of n-step actions while still maintaining the same lookahead, each 1-step action in an action sequence was held constant for an extended amount of time, a multiple of the simulation step Δ. An alternative would be to intelligently compress and prune the lookahead tree, as suggested in (Anthony, Polani, & Nehaniv, 2009) for discrete scenarios, which there allows to extend the horizon by more than an order of magnitude at similar complexity. Here, however, we are going to demonstrate that even the locally informed empowerment with short lookahead horizons is sufficient to treat aforementioned scenarios.

Results for inverted pendulum: Figure 5 (top row) shows a phase plot of the behavior that results from starting in the initial condition (pole hanging vertically down) and following 3-step empowerment (and thus $N_n = 5 \times 5 \times 5$ n-step actions) for a period of 20 seconds with state transition noise $\mathbf{\Sigma} =$

$0.01\mathbf{I}_{2\times2}$ (where $\mathbf{I}_{n\times n}$ denotes the $n \times n$ identity matrix). The plot demonstrates that: (1) empowerment alone makes the agent drive up the pendulum and successfully balance it indefinitely; (2) the agent accomplishes the goal without being explicitly "told" to do so; and (3) the trajectory shows that this happens in a straight and direct way, without wasting time (and consistently so). Note that empowerment only "illuminates" the local potential future of the current state and has no access to the global value of the trajectory as opposed to optimal control methods where implicitly global information about the goal states must be propagated back throughout the system model for the controller to take the right decision.

To compare these results with a different angle, we reformulate the problem as a minimum-time optimal control task: as opposed to before, we now assume that the agent has an explicit, externally specified goal (swinging up the pendulum as fast as possible and successfully balancing it afterwards). A step-wise cost function which implements this goal is given by

$$g(\mathbf{x}_t, u_t) = \begin{cases} -\|\mathbf{x}_t\|^2 & \text{if } \|\mathbf{x}_t\| < 0.1 \\ -1 & \text{otherwise} \end{cases} \tag{12}$$

Since the dimensionality of the state space is low, we can use dynamic programming (value iteration with grid-based interpolation) to directly determine the *optimal* behavioral policy, where optimal means choosing actions such that the accumulated costs from Eq. (12) are minimized among all possible behaviors (Sutton & Barto, 1998). Comparing the results in Figure 5 (bottom row) from using dynamic programming as opposed to using the empowerment heuristic in Figure 5 (top row) shows the remarkable result that with empowerment we achieve nearly the same behavior as with optimal control. The result is remarkable because, unlike the optimal value function, which through the underlying cost function is tied to a particular goal, empowerment is a generic heuristic that operates on the innate characteristics of the dynamics of the system alone.
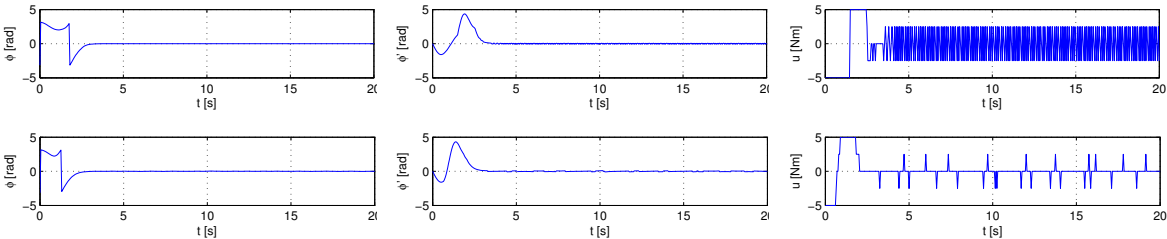
Figure 5: Inverted pendulum: phase plot of $\phi, \dot{\phi}$ and control u when following the greedy policy with respect to: empowerment (top row); dynamic programming (bottom row).

Results for bicycle: For the more complex bicycle domain, the goal is to keep the bicycle going forward by preventing it from falling over to one side or the other; when the angle from the vertical axis, ω, deviates too much from zero (that is, is greater than $\frac{12\pi}{180}$) the bicycle is considered to have fallen. Whenever this happens, the bicycle stops moving forward, and no matter what action the agent takes, the successor state will be the same for all future time steps (absorbing state), and consequently empowerment will be zero.

Here we examine the behavior of empowerment for different initial conditions of the bicycle: we ran different trials by varying the angle ω in the interval $\frac{-10\pi}{180}, \frac{-8\pi}{180}, \ldots, \frac{+8\pi}{180}, \frac{+10\pi}{180}$, and $\dot{\omega}$ in the interval $\frac{-30\pi}{180}, \frac{-25\pi}{180}, \ldots, \frac{+25\pi}{180}, \frac{+30\pi}{180}$; α and $\dot{\alpha}$ were initially zero in all cases. We employ 3-step empowerment (and thus $N_n = 5 \times 5 \times 5$ possible n-step actions) where each 1-step action in an action sequence is held constant for 4 simulation steps, and state transition noise $\boldsymbol{\Sigma} = 0.001\mathbf{I}_{4\times4}$. Figure 6 (right) shows that empowerment is able to keep the bicycle stable for a wide range of initial conditions; dots indicate that the bicycle successfully kept going forward for 20 seconds, stars indicate that it did not. Note that

in many cases of failure, it would actually have been physically impossible to prevent the bicylce from falling; for example, when the bicycle already is strongly leaning to the left and further has velocity pointing to the left. Also note that the column corresponding to zero angle shows an outlier[5]; while empowerment was able to balance the bicycle for $\dot{\omega} = \frac{-20\pi}{180}$, it was not for $\dot{\omega} = \frac{+20\pi}{180}$. Figure 6 (left) shows a phase plot when starting from the initial condition $\omega = \frac{8\pi}{180}$; as we can see, empowerment keeps the bicycle stable and brings the system close to the point $(0, 0, 0, 0)$, from where it can be kept stable indefinitely.
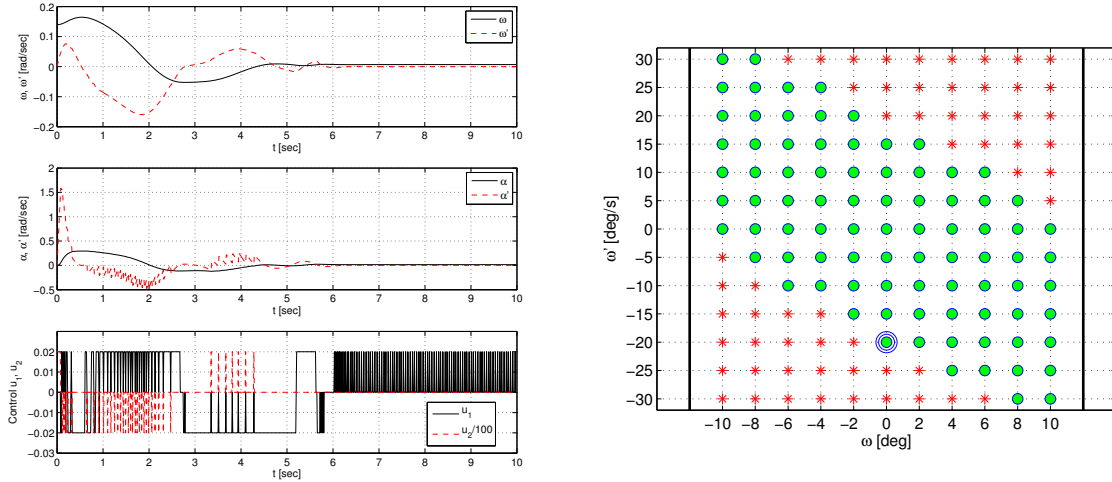
Figure 6: Bicycle: (left side) phase plot of state variables $\omega, \dot{\omega}$ (upper panel), $\alpha, \dot{\alpha}$ (middle panel), and controls u_1, u_2 (lower panel) when starting from state $\left(\frac{8\pi}{180}, 0, 0, 0\right)$ and following the empowerment-based policy; (right side) shows how empowerment is able to successfully balance the bicycle for a large variety of initial conditions; the black vertical bars indicate failure states; that is, the value of angle ω from which failure can no longer be avoided.

Results for acrobot: For the highly challenging acrobot we require a deeper lookahead: here we consider 5-step empowerment (and thus $N_n = 3 \times 3 \times 3 \times 3 \times 3$ possible n-step actions), where each 1-step action in an action sequence is held constant for 4 simulation steps, and state transition noise $\Sigma = 0.01\mathbf{I}_{4\times4}$. The phase plot in Figure 8 demonstrates that empowerment then leads to a successful swing-up behavior, approaches the unstable equilibrium, and in particular makes the agent actually balance in the inverted handstand position. Figure 7 illustrates how these numbers translate into the real physical system. Figure 8 (bottom right) shows the corresponding empowerment, that is, it shows for every time step the empowerment value of the state the agent is in; while empowerment does not increase monotonically in every single time step, it increases over the time and reaches the maximum in the handstand position. The vertical bar in the figure indicates the point where the 'balance' action was chosen for the first time as the action with highest empowerment. From this point on, just choosing the 'balance' would have been sufficient; however, the phase plot of the control variable reveals that during this phase, the balance action was not always the one with the highest empowerment.[6] Note that the 'balance' action (see Eq. (16) in the appendix) produces values in the interval $[-1, +1]$ only for states

---

[5]The outlier is a result of inaccuracy produced from Monte-Carlo approximation. Repeating the experiment with a larger number of samples showed that indeed the bicycle can be balanced from both initial conditions. However, note that these initial conditions were already close to the boundary from where balancing becomes impossible, regardless of how many samples are used.

[6]This observation was not due to inaccuracies because of Monte-Carlo approximation. However, while empowerment does not exactly produce the sequence of minimal-time optimal controls, its qualitative behavior is close.
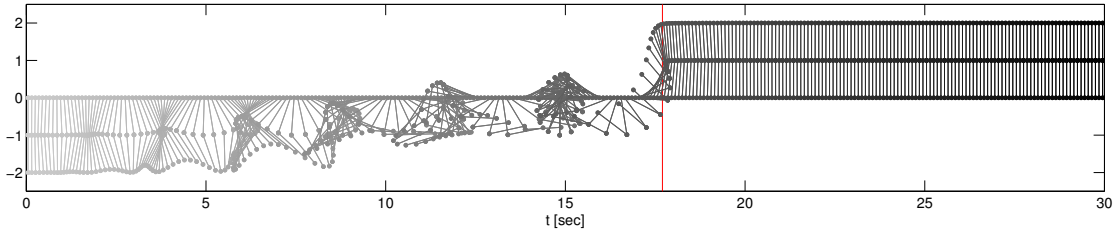
Figure 7: Empowerment alone makes the acrobot swing up, approach the unstable equilibrium, and balance in the inverted handstand position indefinitely.

very close to the handstand position and, because of saturation, behaves like the two other actions $+1$ or -1 otherwise.

5.3 Second scenario: model-learning and exploration

In the second experiment we will discuss a scenario for empowerment which extends its potential applicability; here we are interested in model-learning and using empowerment to extrapolate "intelligently" which part of the state space to explore next. In particular, we will consider the case of *online* model learning; i.e., learning the state transition probabilities from the samples an agent experiences while interacting with the environment (which is more challenging since in general we cannot generate transitions at arbitrary points in the state space and have to make do with the states encountered during a specific – and realistically achievable – run). The key idea here will be to show that with empowerment we can avoid sampling the state space exhaustively, and instead can learn the target behavior from only very few system-agent interactions.

5.3.1 Overview of the learning architecture

An overview of the learning architecture is depicted in Figure 9. The agent consists of two components. One is the model learner $\mathcal{M}_t$, which stores a history of all transitions $\mathcal{D}_t = \{\mathbf{x}_i, a_i, \mathbf{x}'_i\}_{i=1}^t$ seen up to the current time t and which implements multiple GPs to provide 1-step predictions $p(\mathbf{x}_{t+1}|\mathbf{x}_t, a_t, \mathcal{M}_t)$ (Section 4.1) and n-step predictions $p(\mathbf{x}_{t+n}|\mathbf{x}_t, \vec{a}_t^n, \mathcal{M}_t)$ (Section 4.2). The second component is the action selector. Given the current state of the environment, we first determine the successor states under each of the possible 1-step actions using the mean of the predictions from $\mathcal{M}_t$. For each successor state, we then determine their empowerment value (Section 3.4.3) using n-step predictions from $\mathcal{M}_t$. Since the predicted successor states depend on the accuracy of $\mathcal{M}_t$, we adjust their empowerment scores by the uncertainty of the associated 1-step prediction. This uncertainty is taken to be the sum of the individual uncertainties of the state components in Eq. (11). We employ what is called *optimism in the face of uncertainty*: the less certain the system is, the more we want it to perform an exploratory action. Here, we linearly interpolate between the two extremes maximum uncertainty (where we assign $\log N_n$, the upper bound on empowerment) and minimum uncertainty (where we assign the actual empowerment score). The concrete value of the maximum uncertainty, $\beta > 0$, and minimum uncertainty, $\alpha \geq 0$, depend on the hyperparameters of the GPs implementing $\mathcal{M}_t$, for details see (Rasmussen & Williams, 2006). At the end, the agent executes the highest ranked action, observes the outcome and updates the model $\mathcal{M}_t$ accordingly (for performance reasons only every K steps). A summary of the control loop is shown below:

1. **Initialize:**

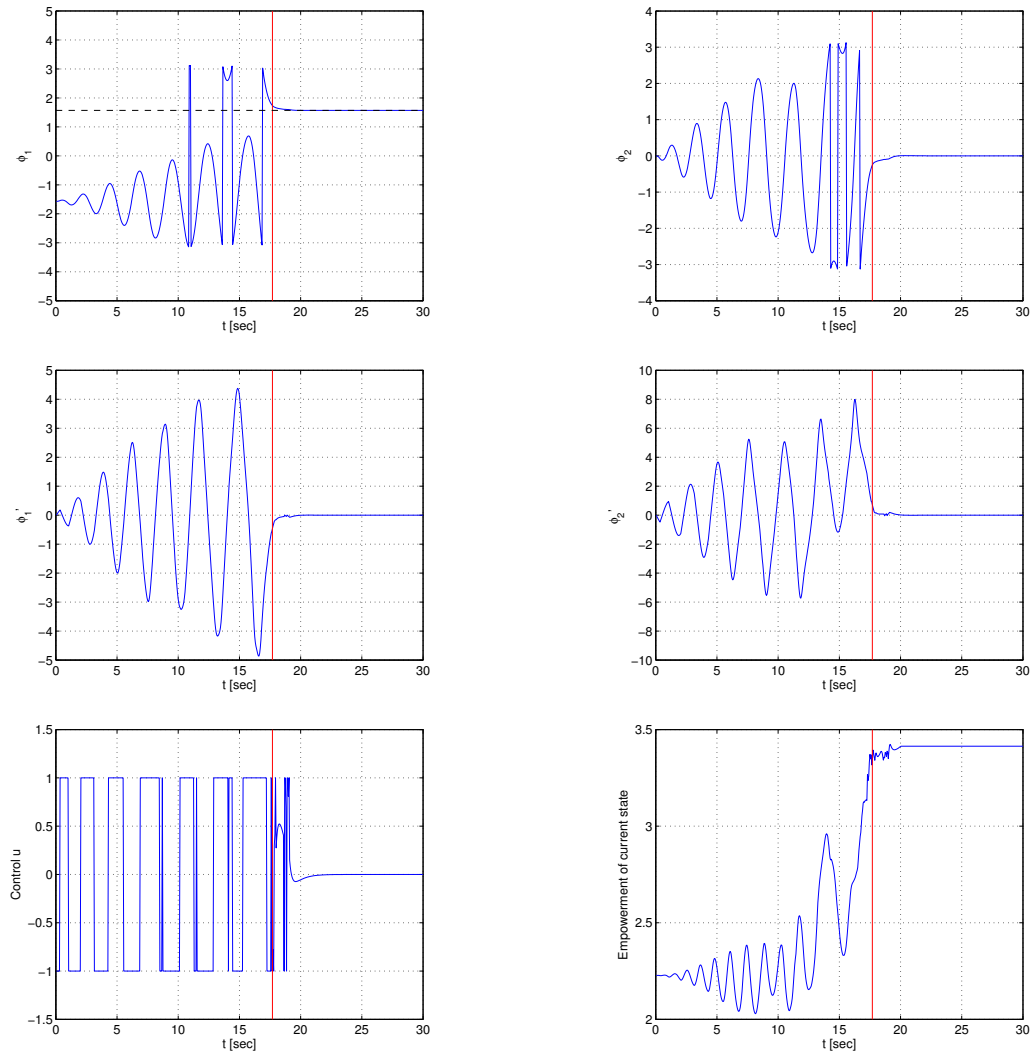   (a) Generate initial transitions $\mathcal{D}_0$.

Figure 8: Acrobot: phase plot when following the empowerment-based policy. The bottom right panel shows the associated empowerment values. The vertical bar shows the first time the 'balance' action was chosen and produced values between the extreme controls −1 and +1.
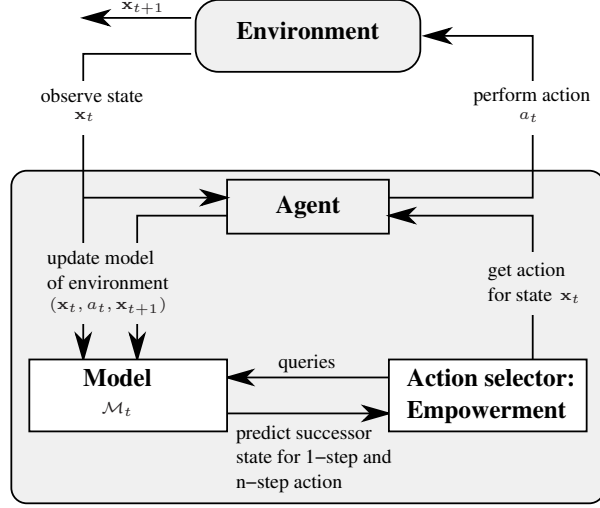
Figure 9: A framework for model-learning and empowerment-based exploration.

    (b) Learn initial model $\mathcal{M}_0$.

2. **Loop:** $t = 1, 2, \ldots$

    (a) Observe current state $\mathbf{x}_t$

    (b) For each 1-step action $\nu = 1, \ldots, N_a$

        i. Compute 1-step successor under ν using $\mathcal{M}_t$ (Section 4.1)

$$p(\mathbf{x}_{t+1}^\nu | \mathbf{x}_t, a_t = \nu, \mathcal{M}_t) = \mathcal{N}(\boldsymbol{\mu}_\nu(\mathbf{x}_t), \boldsymbol{\Sigma}_\nu(\mathbf{x}_t))$$

        ii. Compute n-step empowerment $c_t^\nu := c(\boldsymbol{\mu}_\nu(\mathbf{x}_t))$ (Section 3.4.3) using n-step predictions provided by $\mathcal{M}_t$ (Section 4.2).

        iii. Adjust empowerment scores according to the scalar uncertainty $\operatorname{tr} \boldsymbol{\Sigma}_\nu(\mathbf{x}_t)$ of the 1-step prediction in $\mathbf{x}_t$, linearly interpolating between $\log N_n$ (max uncertainty) and c_t^ν (min uncertainty):

$$\tilde{c}_t^\nu := c_t^\nu + \frac{\operatorname{tr} \boldsymbol{\Sigma}_\nu(\mathbf{x}_t) - \alpha}{\beta - \alpha}(\log N_n - c_t^\nu)$$

        where α and β are the min and max uncertainty values of the predictions (depend on the hyperparameters of $\mathcal{M}_t$)

    (c) Find best action $a_t := \operatorname{argmax}_{\nu=1\ldots N_a} \tilde{c}_t^\nu$

    (d) Execute a_t. Observe $\mathbf{x}_{t+1}$. Store transition $\mathcal{D}_{t+1} = \mathcal{D}_t \cup \{\mathbf{x}_t, a_t, \mathbf{x}_{t+1}\}$.

    (e) Every K steps: update model $\mathcal{M}_t$ using $\mathcal{D}_t$.

5.3.2 Results

For this experiment, we will only consider the inverted pendulum domain for which it will be comparatively easy, because of low dimensionality, to compute the respective optimal behavior. The dynamics of the domain is modified to obtain an episodic learning task: every 500 steps, the state of the system is reset to the initial condition $(\pi, 0)$, and a new episode starts. The action selector computes empowerment using the same parameters as in the previous section, with the difference that now 1-step and

n-step successor states are predicted by the current model. The model-learner is updated (re-trained) every $K = 10$ samples; for the GPs we employ the ARD kernel (Rasmussen & Williams, 2006) with automatic selection of hyperparameters.

For comparison, we consider RMAX (Brafman & Tennenholtz, 2002), a common model-based reinforcement learning algorithm, which also combines exploration, model learning and control, and operates not unlike the learning framework we have described in Section 5.3.1. The main difference is that RMAX is derived from dynamic programming and value iteration and finds agent behavior that optimizes a given performance criterion. The performance criterion, as before, is the explicit cost function Eq. (12), which makes the agent want to reach the goal as fast as possible. For RMAX we have to learn a model both for the transitions of the environment and the cost function. While the former could be done with GPs (same as with empowerment), the latter can not be done by GPs. The reason is that the cost function is flat in every part of the state space except for a very small region about the goal. Since all the initial samples the agent experiences will be from the flat region, a GP would rapidly conclude that the whole cost function is flat; since the uncertainty of the model guides exploration, the GP would predict a -1 cost for all states with very high confidence, and thus the agent would miss the goal for a long time (creating a "needle-in-a-haystack" situation).

As it is usually done for RMAX, we therefore use a grid-based discretization to estimate costs and transitions.[7] Uncertainty of a prediction then depends on whether or not the underlying grid-cell has been visited before. Since in RMAX unvisited states are more attractive than reaching the goal, the agent tends to explore the environment exhaustively before it can behave optimally.

In Figure 10 we compare our empowerment-based exploration with RMAX for various spacings of the underlying grid: we examine division into $25, 50, 75, 100$ cells. Every curve shows the cumulative costs (under cost function Eq. (12)) as a function of episode. Thus every curve has two parts: a transient one where the agent is still learning and acting non-optimally, and a steady-state one where the agent is acting optimally with respect to its underlying bias which is either maximizing empowerment or minimization of costs.

The graph shows two things: (1) the finer the resolution of the grid, the longer it takes RMAX to act optimally. For a grid of size 25, the agent reaches optimal performance after 23 episodes; for a grid of size 50 it needs 60 episodes; for a grid of size 75 it needs 117 episodes; and for a grid of size 100 it needs 165 episodes. On the other hand, empowerment only needs 3 episodes until steady-state behavior is reached. (2) The steady-state performance of empowerment is somewhat worse than that of RMAX, about 56 versus 78. However, this is not at all surprising. Empowerment does not at all consider the externally defined cost function when making decisions, whereas RMAX specifically optimizes agent behavior such that performance with respect to this particular cost function is maximized. Still, behavior under empowerment is close to what we would achieve by explicitly optimizing a cost function; however, with empowerment, the agent can learn this behavior much faster since it does not have to exhaustively explore the state space (it only has to explore the state space to the extent of learning an accurate model for state transitions).

Figure 11 shows in more detail how empowerment drives the agent to visit only the relevant part of the state space. The figure compares, for empowerment and RMAX with grid spacing 25, what state-action pairs are visited during learning at various points in time (note that in both cases the model learner treats actions independently from each other and does not generalize between them). The plots show that, for the empowerment-based agent, the GP-based model-learner can accurately predict state transitions after having seen only few very samples. As the accuracy of predictions goes up, uncertainty of predictions goes down, as the GP becomes more confident about what it does. Low uncertainty in turn means that the agent no longer takes exploratory actions, but instead chooses the one with the highest empowerment. If the learned model is accurate enough, this is as good as knowing the true transitions

---

[7]The value iteration part of RMAX is also carried out with interpolation on a high-resolution grid. However, the details of this step are of no concern in this paper, and the performace comparison we make is unaffected by it.
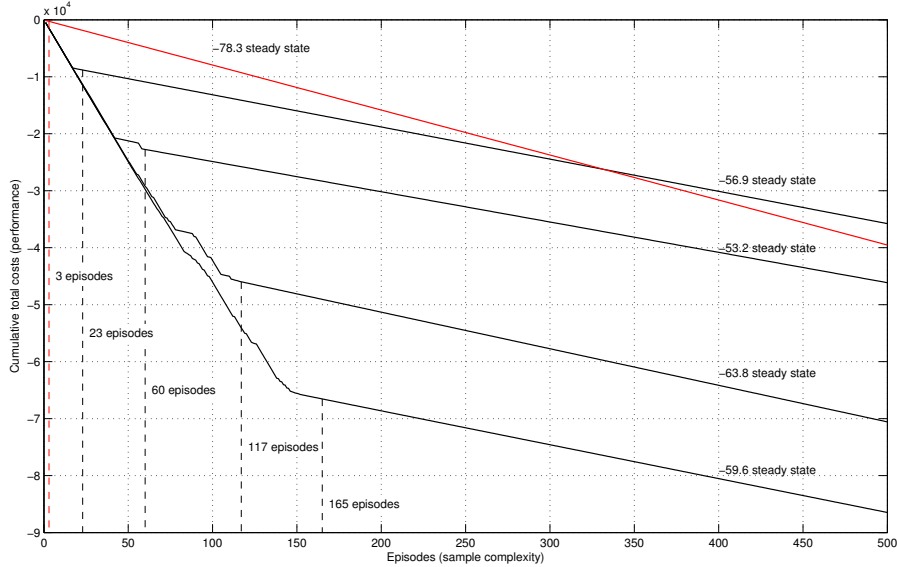
Figure 10: Exploration and model-based learning in the inverted pendulum domain. The plot compares both the sample efficieny and ultimate performance of the learned behavior for empowerment with GPs (top curve) and RMAX with different levels of discretization: grid sizes 25, 50, 75, 100 (bottom curves).

function and the agent behaves accordingly (compare with model-based results in Section 5.2). As the plot shows, here this happens very soon, right within the first episode. RMAX on the other hand has to exhaustively sample the state-action space and essentially visit every grid-cell under each action. Thus it takes much longer to even reach the goal region and then learn the desired behavior.

6 Discussion

A central question that we need to address is: why does empowerment actually carry out intuitively desirable behaviour? In previous work, it has been shown that this property is not spurious, but actually reappears in a number of disparate scenarios (Klyubin et al., 2005a; Klyubin, Polani, & Nehaniv, 2005b; Klyubin et al., 2008; Anthony, Polani, & Nehaniv, 2008; Anthony et al., 2009).

On the other hand, one can clearly create a scenario where empowerment will fail to match the externally imposed goal: imagine for instance the inverted pendulum task, where the target state is some oblique angle $\phi \neq 0$, different from the upright position. Even if the position is sustainable (we remind the reader that the task was underactuated), that position would clearly not match the state an empowerment maximization strategy will try to attain. Nevertheless, the task of placing the pole in an arbitrary oblique position $\phi \neq 0$ strikes one as unnatural if nothing else is specified in the task. In other words, balancing the inverted pendulum seems to be the most unbiased, natural task to do in that scenario.

However, of course, there are scenarios where preferred outcomes do not naturally arise from the system dynamics. The most obvious examples are, e.g., mazes where one needs to reach a particular goal state. This goal state can obviously be arbitrary, and selected independently from the actual dynamics/topology of the system. Even in such scenarios, empowerment still mimics/approximates the graph-theoretic notion of *centrality* (Anthony et al., 2008); this means that empowerment maximization will place the agent (approximately) at a location in the world from which the expected distance to a

(a) Empowerment: 250 transitions

(b) RMAX: 250 transitions

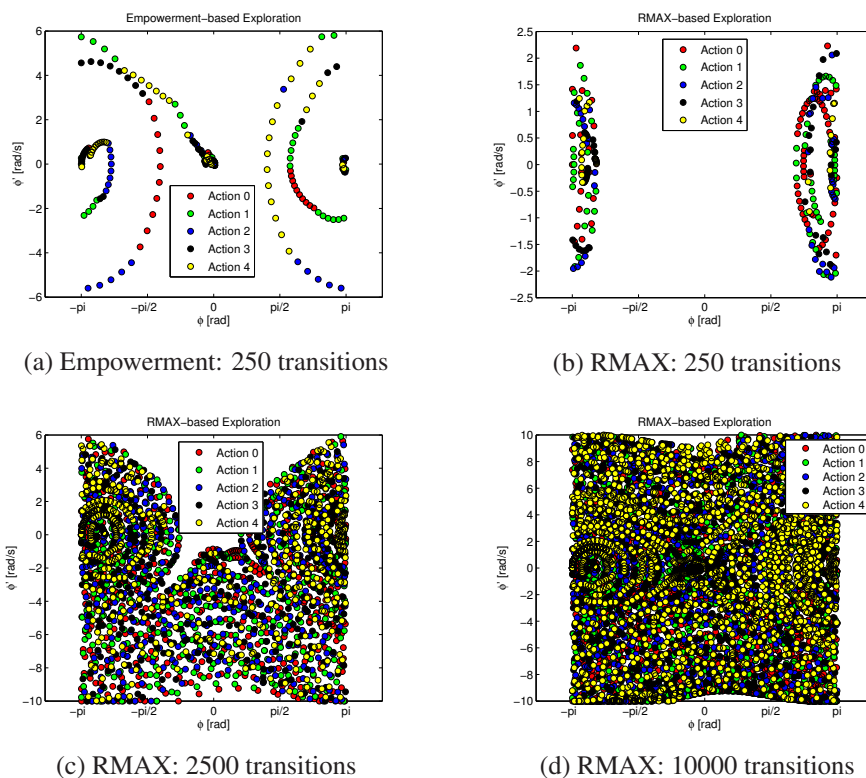(c) RMAX: 2500 transitions

(d) RMAX: 10000 transitions

Figure 11: Distribution of visited state-action pairs for empowerment and RMAX. Empowerment reaches the goal region around the point $(0, 0)$ after about 250 transitions right in the very first episode, whereas RMAX needs more than ten times as long. With empowerment, the agent only has to explore limited parts of the state-action space until the model is learned. Under RMAX, in order to also learn the external cost function, the state-action space needs to be sampled exhaustively.

randomly specified goal state will be minimal. In other words, it is "the best guess" where the agent should place itself in expectation of a yet unknown goal, assuming one wishes to minimize the number of steps to the goal[8].

However, the performance in our scenarios is even better than that in that the natural goals that one would impose a priori here seem to be anticipated by what empowerment is trying to maximize. Now, all the considered scenarios have one thing in common: they are survival-type scenarios. The agent aims to stay "alive" and to move away from "death" states as far as possible (we adopt here an argument that is related to Friston's free energy model of cognition which has been brought up in (Friston, Kilner, & Harrison, 2006; Friston, 2009)).

What makes this particularly interesting in the context of continuous systems which are our point of concern in the present paper is that the smoothness of the system informs the local empowerment gradients around the agent's state of where the most "alive" states are (and many dynamical systems have this property). But even discrete transition graphs display — in somewhat structured scenarios like grid-worlds or small-world networks (Anthony et al., 2008) — this property that the attraction basins of global or good local empowerment optima are visible from some distance. This is particularly striking

---

[8]We completely omit the discussion of the case when different actions have different costs for different states — this obviously forces one to resort to the full-fledged dynamic programming formalism. However, this is clearly a case where the specification of environmental structure and dynamics are not sufficient for the characterization of the task and the reward structure needs to be explicitly specified. The issues of balancing explicit rewards and the information-theoretic costs of decision making are intricate and are discussed in detail elsewhere (Tishby & Polani, 2010).

since empowerment seems to correlate well with measures for dominating states in graphs which have been hand-crafted for that purpose (Anthony et al., 2008).

Where empowerment maximization coincides with the "natural" optimal control task, it computes *local* gradients towards the right direction as opposed to optimal control/dynamic programming which implicitly require a global picture of where the goal states are. It is an open question what properties are required from a system to provide these relatively large attraction basins of empowerment maxima that are visible in local empowerment gradients. This property seems to be present in continuous environments and in environments with some degree of globally homogeneous structures (Anthony et al., 2008).

Different from that are, however, novel degrees of freedom which form "gateways" in the state space in that they are particular locations in the world that grant access to new subregions in the state space (implying novel ways of interacting with the environment) that are otherwise inaccessable from the majority of states. A prime example is the taxi domain from Section 2, where the actions of picking up and dropping off a passenger open new degrees of freedom, but only at specific locations in the maze (another example is the "box pushing" scenario where an agent's empowerment increases close to a pushable box due to the increased number of options (Klyubin et al., 2005a)). Such gateways are usually irregular occurences in the state space and will typically only be detected by empowerment if they are in reach of the action horizon. Still, intelligent action sequence extension algorithms such as suggested in (Anthony et al., 2009) may provide recourse and larger effective action horizons even in these cases. However, the examples studied in this paper do not involve any such gateways and all require only relatively short horizons by virtue of their smooth structure. This suggests that for the significant class of dynamic control problems empowerment may provide a purely local exploration and behaviour heuristic which identifies and moves towards particularly "interesting" areas; the present paper furthermore demonstrates how this can be implemented in an efficient on-line fashion.

7 Summary

This paper has discussed empowerment, an information-theoretic quantity that measures, for any agent-environment system with stochastic transitions, the extent to which the agent can influence the environment by its actions. While earlier work with empowerment has already shown its various uses in a number of different domains, empowerment calculation was previously limited to the case of small-scale and discrete domains where state transition probabilities were assumed to be known by the agent. The main contribution of this paper is to relax both assumptions. First, this paper extends calculation of empowerment to the case of continuous vector-valued state spaces. Second, we discuss an application of empowerment to exploration and online model-learning where we no longer assume that the precise state transition probabilities are a priori known to the agent. Instead, the agent has to learn them through interacting with the environment.

By addressing vector-valued state-spaces and model-learning, this paper already significantly advances the applicability of empowerment to real-world scenarios. Still, from a computational point of view, open questions remain. One question in particular is how to best deal with continuous, vector-valued action spaces – so far we assumed in this paper that the action space could be discretized. However, for higher dimensional action spaces (which are common in robotic applications), a naive discretization will soon become infeasible.

Acknowledgments

Table 1: Physical parameters of the inverted pendulum domain

Symbol	Value	Meaning
g	$9.81\ [m/s^2]$	gravitation
m	$1\ [kg]$	mass of link
l	$1\ [m]$	length of link
μ	0.05	coefficient of friction

A Dynamic model of the inverted pendulum

Refer to the schematic representation of the inverted pendulum given in Figure 4. The state variables are the angle measured from the vertical axis, $\phi(t)$ [rad], and the angular velocity $\dot{\phi}(t)$ [rad/s]. The control variable is the torque $u(t)$ [Nm] applied, which is restricted to the interval $[-5, 5]$. The motion of the pendulum is described by the differential equation:

$$\ddot{\phi}(t) = \frac{1}{ml^2}\Big(-\mu\dot{\phi}(t) + mgl\sin\phi(t) + u(t)\Big). \tag{13}$$

The angular velocity is restricted via saturation to the interval $\dot{\phi} \in [-10, 10]$. The values and meaning of the physical parameters are given in Table 1.

The solution to the continuous-time dynamic equation in Eq. (13) is obained using a Runge-Kutta solver. The time step of the simulation is 0.2 sec, during which the applied control is kept constant. The 2-dimensional state vector is $\mathbf{x}(t) = \big(\phi(t), \dot{\phi}(t)\big)^T$, the scalar control variable is $u(t)$. Since our algorithm in Section 3.4.3 allows us to compute empowerment only for a finite set of possible 1-step actions, we discretized the continuous control space into 5 discrete action choices $a \in \{-5, -2.5, 0, 2.5, 5\}$.

B Dynamic model of the acrobot

Refer to the schematic representation of the acrobot domain given in Figure 4. The state variables are the angle of the first link measured from the horizontal axis, $\theta_1(t)$ [rad], the angular velocity $\dot{\theta}_1(t)$ [rad/s], the angle between the second link and the first link $\theta_2(t)$ [rad], and its angular velocity $\dot{\theta}_2(t)$ [rad/s]. The control variable is the torque $\tau(t)$ [Nm] applied at the second joint. The dynamic model of the acrobot system is (Spong, 1995):

$$\ddot{\theta}_1(t) = -\frac{1}{d_1(t)}\big(d_2(t)\ddot{\theta}_2(t) + \phi_1(t)\big) \tag{14}$$

$$\ddot{\theta}_2(t) = \frac{1}{m_2 l_{c2}^2 + I_2 - \frac{d_2(t)^2}{d_1(t)}}\left(\tau(t) + \frac{d_2(t)}{d_1(t)}\phi_1(t) - m_2 l_1 l_{c2}\dot{\theta}_1(t)^2\sin\theta_2(t) - \phi_2(t)\right) \tag{15}$$

Table 2: Physical parameters of the acrobot domain

Symbol	Value	Meaning
g	$9.8\,[m/s^2]$	gravitation
m_i	$1\,[kg]$	mass of link i
l_i	$1\,[m]$	length of link i
l_{ci}	$0.5\,[m]$	length to center of mass of link i
I_i	$1\,[kg \cdot m^2]$	moment of inertia of link i

where

$$d_1(t) := m_1 l_{c1}^2 + m_2\big(l_1^2 + l_{c2}^2 + 2l_1 l_{c2}\cos\theta_2(t)\big) + I_1 + I_2$$

$$d_2(t) := m_2\big(l_{c2}^2 + l_1 l_{c2}\cos\theta_2(t)\big) + I_2$$

$$\phi_1(t) := -m_2 l_1 l_{c2}\dot{\theta}_2(t)^2\sin\theta_2(t) - 2m_2 l_1 l_{c2}\dot{\theta}_2(t)\dot{\theta}_1(t)\sin\theta_2(t) + \big(m_1 l_{c1} + m_2 l_1\big)g\cos\theta_1(t) + \phi_2(t)$$

$$\phi_2(t) := m_2 l_{c2}g\cos\big(\theta_1(t) + \theta_2(t)\big).$$

The angular velocities are restricted via saturation to the interval $\theta_1 \in [-4\pi, 4\pi]$, and $\theta_2 \in [-9\pi, 9\pi]$. The values and meaning of the physical parameters are given in Table 2; we used the same parameters as in (Sutton & Barto, 1998).

The solution to the continuous-time dynamic equations in Eqs. (14)-(15) is obained using a Runge-Kutta solver. The time step of the simulation is 0.2 sec, during which the applied control is kept constant. The 4-dimensional state vector is $\mathbf{x}(t) = \big(\theta_1(t), \theta_2(t), \dot{\theta}_1(t), \dot{\theta}_2(t)\big)^T$, the scalar control variable is $\tau(t)$.

The motor was allowed to produce torques τ in the range $[-1, 1]$. Since our algorithm in Section 3.4.3 allows us to compute empowerment only for a finite set of possible 1-step actions, we discretized the continuous control space. Here we use three actions: the first two correspond to a bang-bang control and take on the extreme values -1 and $+1$. However, a bang-bang control alone does not allow us to keep the acrobot in the inverted handstand position, which is an unstable equilibrium. As a third action, we therefore introduce a more complex balance-action, which is derived via LQR. First, we linearize the acrobot's equation of motion about the unstable equilibrium $(-\pi/2, 0, 0, 0)$, yielding:

$$\dot{\mathbf{x}}(t) = \mathbf{A}\mathbf{x}(t) + \mathbf{B}\mathbf{u}(t),$$

where, after plugging in the physical parameters of Table 2,

$$\mathbf{A} = \begin{bmatrix} 0 & 0 & 1 & 0 \\ 0 & 0 & 0 & 1 \\ 6.21 & -0.95 & 0 & 0 \\ -4.78 & 5.25 & 0 & 0 \end{bmatrix}, \quad \mathbf{B} = \begin{bmatrix} 0 \\ 0 \\ -0.68 \\ 1.75 \end{bmatrix}, \quad \mathbf{x}(t) = \begin{bmatrix} \theta_1(t) - \pi/2 \\ \theta_2(t) \\ \dot{\theta}_1(t) \\ \dot{\theta}_2(t) \end{bmatrix} \quad \mathbf{u}(t) = \tau(t).$$

Using MATLAB, an LQR controller was then computed for the cost matrices $\mathbf{Q} = \mathbf{I}_{4\times4}$ and $\mathbf{R} = 1$, yielding the state feedback law

$$\mathbf{u}(t) = -\mathbf{K}\mathbf{x}(t), \tag{16}$$

with constant gain matrix $\mathbf{K} = [-189.28, -47.46, -89.38, -29.19]$. The values resulting from Eq. (16) were truncated to stay inside the valid range $[-1, 1]$. Note that the LQR controller works as intended and produces meaningful results only when the state is already in a close neighborhood of the handstand state; in particular, it is incapable of swinging up and balancing the acrobot on its own from the initial state $(0, 0, 0, 0)$.

Table 3: Physical parameters of the bicycle domain

Symbol	Value	Meaning
g	$9.81\ [m/s^2]$	gravitation
v	$10/3.6\ [m/s]$	constant speed of the bicycle
h	$0.94\ [m]$	height from ground of the common bicycle-rider center of mass
l	$1.11\ [m]$	distance between front and back tire at the point where they touch the ground
r	$0.34\ [m]$	radius of a tire
d_{CM}	$0.3\ [m]$	vertical distance between the bicycle's and rider's center of mass
c	$0.66\ [m]$	horizontal distance between front tire and common center of mass
M_c	$15\ [kg]$	mass of the bicycle
M_d	$1.7\ [kg]$	mass of a tire
M_r	$60\ [kg]$	mass of the rider

C Dynamic model of the bicycle

Refer to the schematic representation of the bicycle domain given in Figure 4. The state variables are the roll angle of the bicycle measured from the vertical axis, $\omega(t)$ [rad], the roll rate $\dot{\omega}(t)$ [rad/s], the angle of the handlebar $\alpha(t)$ [rad] (measured from the longitudal axis of the bicycle), and its angular velocity $\dot{\alpha}(t)$ [rad/s]. The control variables are the displacement $\delta(t)$ [m] of the bicycle-rider common center of mass perpendicular to the plane of the bicycle, and the torque $\tau(t)$ [Nm] applied to the handlebar. The dynamic model of the bicycle system is (Ernst et al., 2005):

$$
\ddot{\omega}(t) = \frac{1}{I_{bc}}\Big\{ \sin(\beta(t))(M_c + M_r)gh
$$
$$
- \cos(\beta(t))\Big[\frac{I_{dc}v}{r}\dot{\alpha}(t) + \text{sign}(\alpha(t))v^2\Big(\frac{M_d r}{l}(|\sin(\alpha(t))| + |\tan(\alpha(t))|) + \frac{(M_c + M_r)h}{r_{CM}(t)}\Big)\Big]\Big\} \tag{17}
$$

$$
\ddot{\alpha}(t) = \begin{cases} \frac{1}{I_{dl}}\big(\tau(t) - \frac{I_{dv}}{r}\dot{\omega}(t)\big) & \text{if } |\alpha(t)| \leq \frac{80\pi}{180} \\ 0 & \text{otherwise} \end{cases} \tag{18}
$$

where

$$
\beta(t) := \omega(t) + a\tan\frac{\delta(t) + \omega(t)}{h}, \qquad \frac{1}{r_{CM}(t)} := \begin{cases} \frac{1}{\sqrt{(l-c)^2 + \frac{l^2}{\sin^2(\alpha(t)^2)}}} & \text{if } \alpha(t) \neq 0 \\ 0 & \text{otherwise} \end{cases}.
$$

The steering angle α is restricted to the interval $[\frac{-80\pi}{180}, \frac{80\pi}{180}]$, and whenever this bound is reached the angular velocity $\dot{\alpha}$ is set to 0. The moments of inertia are computed as:

$$
I_{bc} = \frac{13}{3}M_c h^2 + M_r(h + d_{CM})^2 \qquad\qquad I_{dc} = M_d r^2
$$
$$
I_{dv} = \frac{3}{2}M_d r^2 \qquad\qquad I_{dl} = \frac{1}{2}M_d^2
$$

The values and meaning of the remaining physical parameters are given in Table 3.

Roll rate $\dot{\omega}$ and angular velocity $\dot{\alpha}$ are kept in the interval $[-2\pi, 2\pi]$ via saturation; roll angle ω is restricted to $[\frac{-12\pi}{180}, \frac{12\pi}{180}]$. Whenever the roll angle is larger than $\frac{12\pi}{180}$ in either direction, the bicycle is supposed to have fallen. This state is treated as a terminal state by defining all outgoing transitions as

self-transitions, that is, once a terminal state is reached, the system stays there indefinitely, no matter what control is performed. Thus, to keep the bicycle going forward, the bicycle has to be prevented from falling.

The solution to the continuous-time dynamic equations in Eqs. (17)-(18) is obained using a Runge-Kutta solver. The time step of the simulation is 0.2 sec, during which the applied control is kept constant. The 4-dimensional state vector is $\mathbf{x}(t) = \big(\omega(t), \dot{\omega}(t), \alpha(t), \dot{\alpha}(t)\big)^T$, the 2-dimensional control vector is $\mathbf{u}(t) = \big(\delta(t), u(t)\big)^T$. Control variable δ was allowed to vary in $[-0.02, 0.02]$, α was allowed to vary in $[-2, 2]$. Since our algorithm in Section 3.4.3 allows us to compute empowerment only for a finite set of possible 1-step actions, we discretized the continuous control space. As in (Lagoudakis & Parr, 2003), we only consider the following 5 discrete actions: $a_1 = (-0.02, 0), a_2 = (0, 0), a_3 = (0.02, 0), a_4 = (0, -2), a_5 = (0, 2)$.

References

Anthony, T., Polani, D., & Nehaniv, C. (2009). Impoverished empowerment: 'meaningful' action sequence generation through bandwidth limitation. In G. Kampis & E. Szathmry (Eds.), *Proc. european conference on artificial life 2009, budapest.* Springer.

Anthony, T., Polani, D., & Nehaniv, C. L. (2008). On preferred states of agents: how global structure is reflected in local structure. In S. Bullock, J. Noble, R. Watson, & M. A. Bedau (Eds.), *Artificial life xi: Proceedings of the eleventh international conference on the simulation and synthesis of living systems, winchester 5–8. aug.* (pp. 25–32). MIT Press, Cambridge, MA.

Ay, N., Bertschinger, N., Der, R., Güttler, F., & Olbrich, E. (2008). Predictive information and explorative behavior of autonomous robots. *European Physical Journal B – Condensed Matter and Complex Systems*, *63*, 329–339.

Blahut, R. (1972). Computation of channel capacity and rate distortion functions. *IEEE Trans on Information Theory*, *18*(4), 460–473.

Brafman, R., & Tennenholtz, M. (2002). R-MAX, a general polynomial time algorithm for near-optimal reinforcement learning. *JMLR*, *3*, 213–231.

Der, R. (2000). Selforganized robot behavior from the principle of homeokinesis. In H.-M. Groß, K. Debes, & H.-J. Böhme (Eds.), *Proc. workhop soave '2000 (selbstorganisation von adaptivem verhalten)* (Vol. 643, p. 39-46). Ilmenau: VDI Verlag.

Der, R. (2001). Self-organized acqusition of situated behavior. *Theory Biosci.*, *120*, 1-9.

Der, R., Steinmetz, U., & Pasemann, F. (1999). Homeokinesis – a new principle to back up evolution with learning. In M. Mohammadian (Ed.), *Computational intelligence for modelling, control, and automation* (Vol. 55, p. 43-47). IOS Press.

Dieterich, T. G. (1998). The MAXQ method for hierarchical reinforcement learning. In *Proc. of 15th icml.*

Ernst, D., Geurts, P., & Wehenkel, L. (2005). Tree-based batch mode reinforcement learning. *JMLR*, *6*, 503–556.

Friston, K. (2009). The free-energy principle: a rough guide to the brain? *Trends Cogn. Sci.*, *13*(7), 293-301.

Friston, K., Kilner, J., & Harrison, L. (2006). A free energy principle for the brain. *Journal of Physiology-Paris*, *100*, 70-87.

Girard, A., Rasmussen, C. E., Quiñonero-Candela, J., & Murray-Smith, R. (2003). Gaussian process priors with uncertain inputs: Application to multiple-step ahead time series forecasting. In *Nips 15.*

Kaplan, F., & Oudeyer, P.-Y. (2004). Maximizing learning progress: an internal reward system for development. In F. Iida, R. Pfeifer, L. Steels, & Y. Kuniyoshi (Eds.), *Embodied artificial intelligence* (Vol. 3139, p. 259-270). Springer.

Klyubin, A. S., Polani, D., & Nehaniv, C. L. (2005a). All else being equal be empowered. In *Advances in artificial life, european conference on artificial life (ecal 2005)* (Vol. 3630, p. 744-753). Springer.

Klyubin, A. S., Polani, D., & Nehaniv, C. L. (2005b). Empowerment: A universal agent-centric measure of control. In *Proc. ieee congress on evolutionary computation, 2-5 september 2005, edinburgh, scotland (cec 2005)* (p. 128-135).

Klyubin, A. S., Polani, D., & Nehaniv, C. L. (2008). Keep your options open: An information-based driving principle for sensorimotor systems. *PLoS ONE.*

Lagoudakis, M. G., & Parr, R. (2003). Least-squares policy iteration. *JMLR*, *4*, 1107–1149.

Lungarella, M., Pegors, T., Bulwinkle, D., & Sporns, O. (2005). Methods for quantifying the information structure of sensory and motor data. *Neuroinformatics*, *3*(3), 243-262.

Lungarella, M., & Sporns, O. (2005). Information self-structuring: Key principle for learning and

development. In *Proceedings of 4th ieee international conference on development and learning* (p. 25-30).

Lungarella, M., & Sporns, O. (2006). Mapping information flow in sensorimotor networks. *PLoS Computational Biology*, *2*(10).

Prokopenko, M., Gerasimov, V., & Tanev, I. (2006). Evolving spatiotemporal coordination in a modular robotic system. In S. Nolfi et al. (Eds.), *From animals to animats 9: 9th international conference on the simulation of adaptive behavior (sab 2006), rome, italy* (Vol. 4095, p. 558-569). Berlin, Heidelberg: Springer.

Quiñonero-Candela, J., Rasmussen, C. E., & Williams, C. K. I. (2007). Approximation methods for gaussian process regression. In L. Bottou, O. Chapelle, D. DeCoste, & J. Weston (Eds.), *Large scale learning machines* (pp. 203–223). MIT Press.

Rasmussen, C. E., & Williams, C. K. I. (2006). *Gaussian processes for machine learning*. MIT Press.

Schmidhuber, J. (1991). A possibility for implementing curiosity and boredom in model-building neural controllers. In *Proc. int. conf. simulation of adap behavior: From animals to animats.*

Singh, S., Barto, A. G., & Chentanez, N. (2005). Intrinsically motivated reinforcement learning. In *Nips 17*.

Spong, M. (1995). The swing up control problem for the acrobot. *IEEE Control Systems Magazine*, *15*, 49–55.

Sporns, O., & Lungarella, M. (2006). Evolving coordinated behavior by maximizing information structure. In L. M. Rocha, M. Bedau, D. Floreano, R. Goldstone, A. Vespignani, & L. Yaeger (Eds.), *Proc. artificial life x* (pp. 323–329).

Steels, L. (2004). The autotelic principle. In F. Iida, R. Pfeifer, L. Steels, & Y. Kuniyoshi (Eds.), *Embodied artificial intelligence: Dagstuhl castle, Germany, July 7-11, 2003* (Vol. 3139, pp. 231–242). Berlin: Springer Verlag.

Still, S. (2009). Information theoretic approach to interactive learning. *EPL*, *85*, 28005.

Sutton, R., & Barto, A. (1998). *Reinforcement learning: An introduction*. MIT Press.

Tishby, N., & Polani, D. (2010). Information theory of decisions and actions. In V. Cutsuridis, A. Hussain, & J. Taylor (Eds.), *Perception-action cycle: Models, architecture and hardware.* Springer. (In Press)

Zahedi, K., Ay, N., & Der, R. (2010). Higher coordination with less control — a result of information maximization in the sensorimotor loop. *Adaptive Behaviours*, *18*(3-4), 338-355.